GDR STIC-Santé : Biomécanique des Tissus Mous, Lyon 26 Novembre 2009

Caractérisation exérimentale et modélisation de tissus biologiques

remy.willinger@imfs.u-strasbg.fr

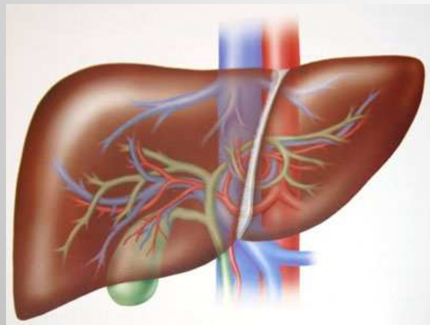

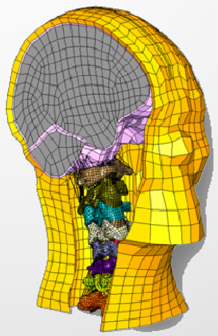

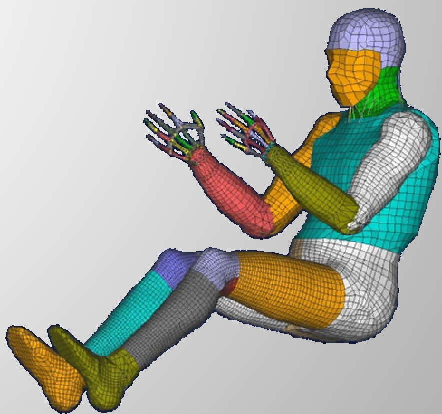

Rémy Willinger[a]

University of Strasbourg, IMFS-CNRS, Strasbourg, France

Introduction:

- Présentation générale des modèles
- *Methodes expérimentales*
    - *Rhéométrie*
    - *Elastographie par RMN*
    - *Elastographie impulsionnelle*
- *Matière hépathique*
    - *In vivo*
    - In vitro
- *Matière cérébrale*
    - Caractérisation et modélisation
    - Limites de tolérance au choc
- Développements futurs

Correlation between liver mechanical characteristics and physiological functions

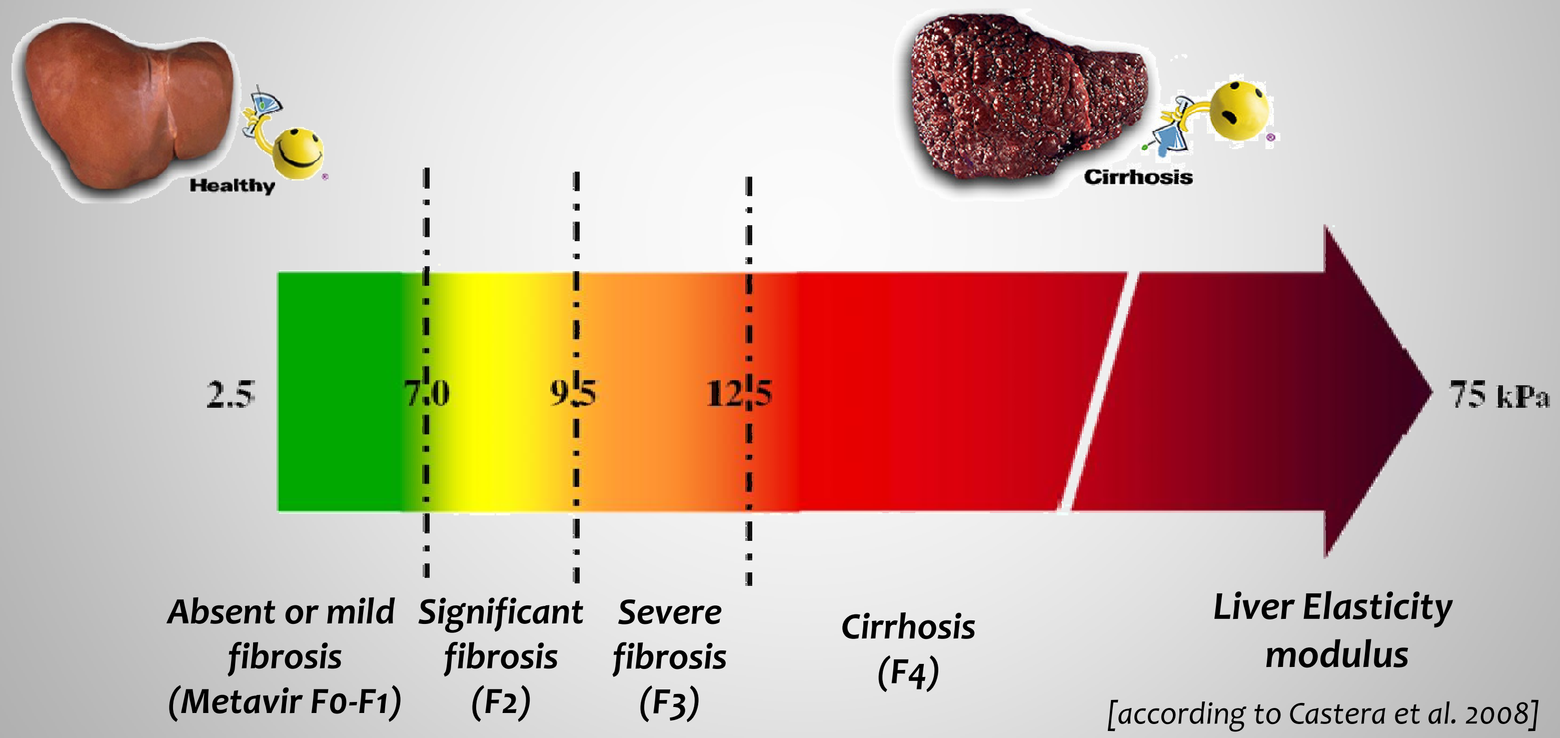

Biomécanique du traumatisme crânio-cérébral et cervical

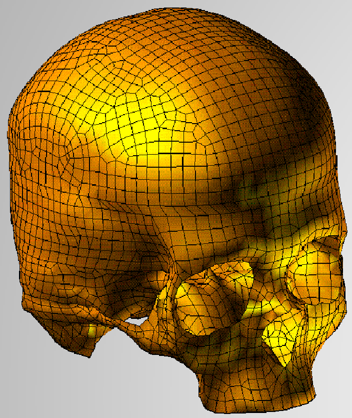

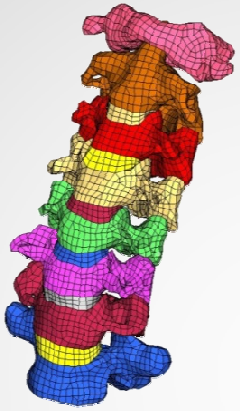

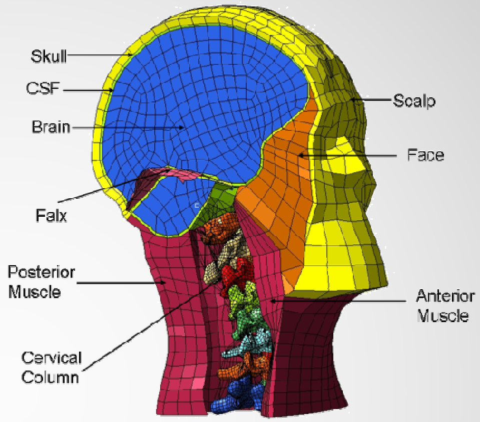

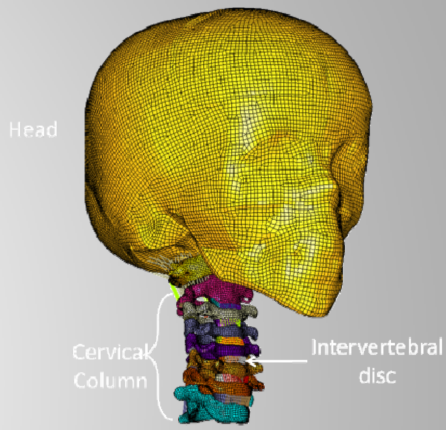

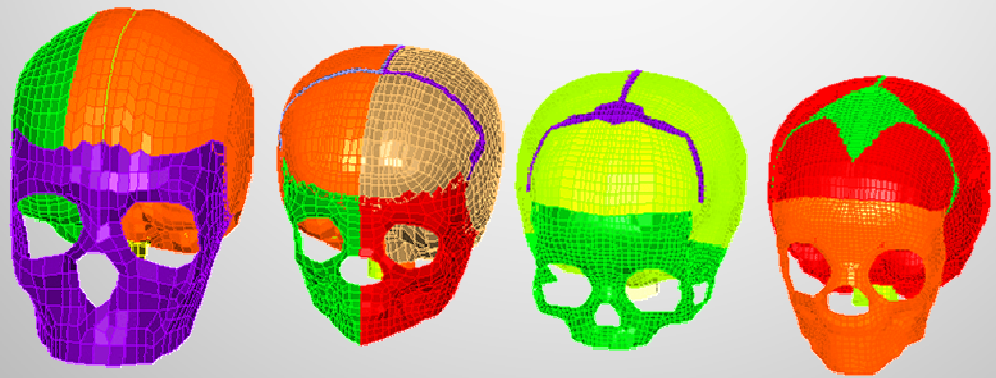

Choix des modèles

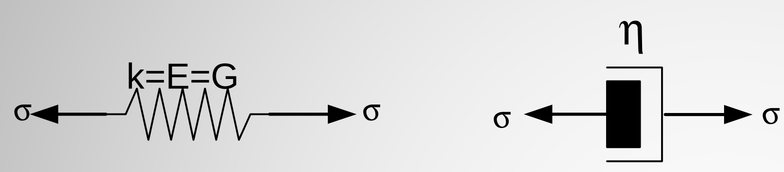

-élément ressort-

-élément amortisseur-

Fig.2-4: Les éléments de base d'un modèle mécanique.

$$\sigma = E\varepsilon$$

$$\sigma = G\gamma$$

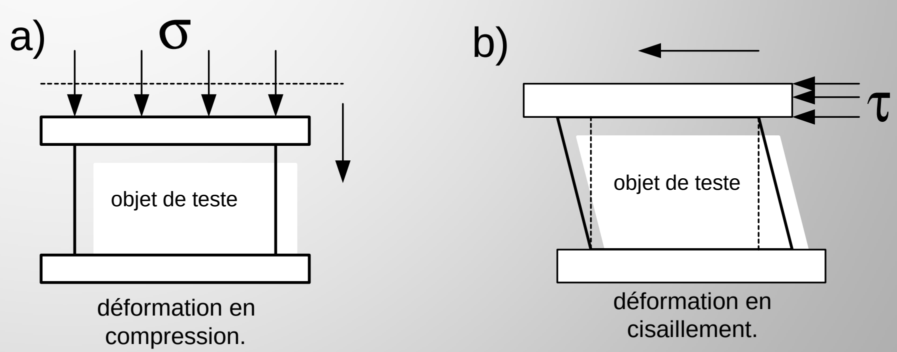

Fig. 2-2: les deux types de déformation de base .

Choix des modèles

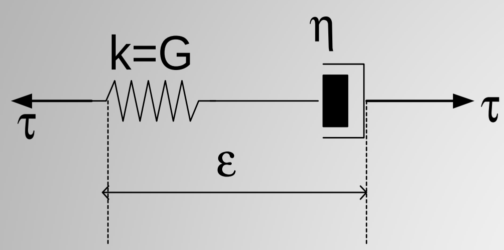

Fig.2-5: Le Modèle de Maxwel (M)

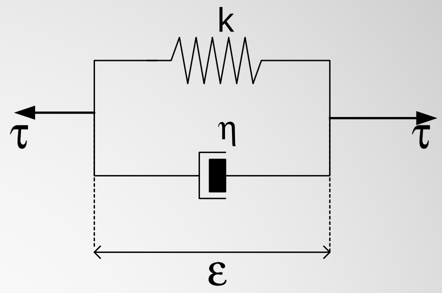

Fig.I-4: Modèle de Kelvin voight (K.V.).

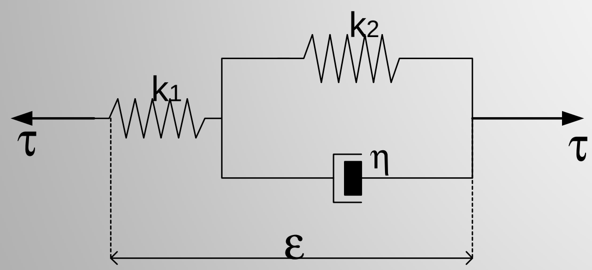

Fig.I-5: Modèle de Maxwel-Kelvin voight (M.KV).

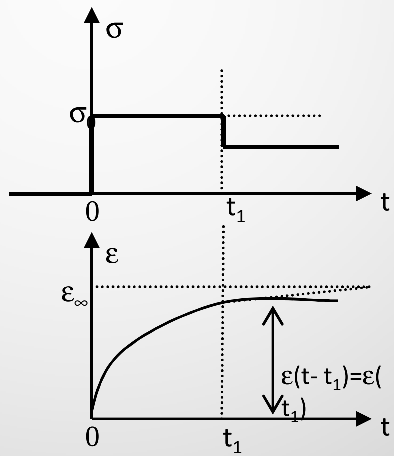

Fig.2-10 : la réponse en fluage du modèle de Kelvin-voight

Choix des modèles

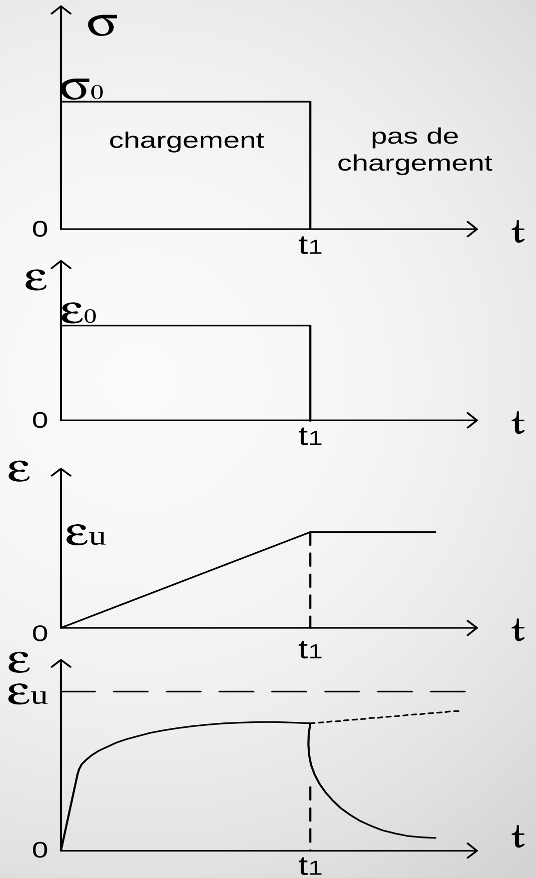

a)

- matériau élastique -

b)

- matériau visqueux -

c)

- matériau viscoélastique -

Fig. 2-1: les trois comportements(élastique, visqueux et viscoélastique) des matériaux.

Méthodes expérimentales

$$\sigma = \sigma_0 \exp(i\omega t + \delta)$$

$$\gamma = \gamma_0 \exp(i\omega t)$$

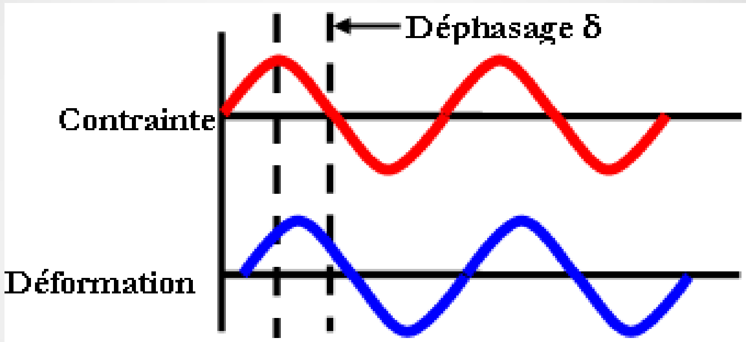

$$G^* = G' + iG''$$

$$G' = \frac{\sigma_0}{\gamma_0}\cos\delta$$

$$G'' = \frac{\sigma_0}{\gamma_0}\sin\delta$$

$$\frac{G''}{G'} = \tan\delta$$

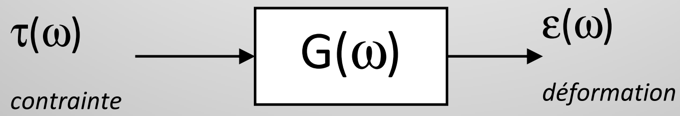

Existing Methodologies

In vivo - **non-invasive** technique

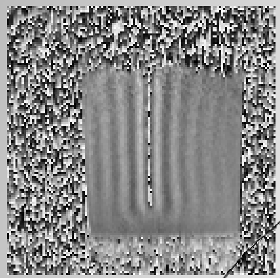

Imaging elastography

Magnetic Resonance Elastography

Ultrasound-based Transient Elastography

Indentation tests

In vivo - **invasive** technique

Rheometric tests

In vitro – **Well known** and validated method

Rhéométrie classique
(DMA)

Dynamic Mechanical Analysis (DMA)

- *In vitro* Dynamical Mechanical Analysis in shear
- G' & G'' (0.1Hz to 10Hz)
- Small deformations: 0.1% strain (linearity)

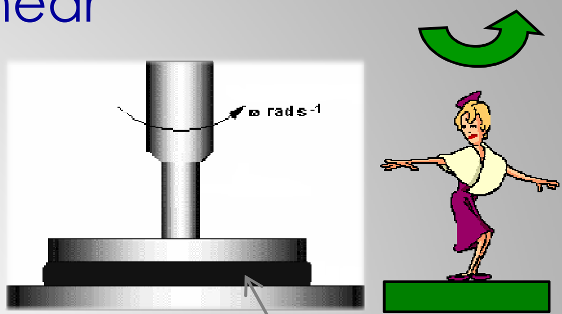

Organ

Cut samples

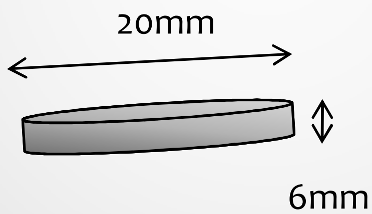

AR 2000 rheometer (TA-Instrument, New Castle, DE)

Synthèse

La rhéométrie : Le rhéomètre

AR 2000 : rhéomètre à contrainte contrôlée

Géométrie : plane

Hypothèses de travail : tissue étudié dans le domaine de viscoélasticité linéaire

(petites déformations)

Paramètres enregistrés : G', G'', raw phase

Lien entre les deux méthodes $G = \sqrt{G'^2 + G''^2}$

$E = 3\rho V_S^2 = 3G$ Hypothèse d'un matériau purement élastique

Elastographie par RMN

The Magnetic Resonance Elastography system

MRI System (0.1T magnets)

Mechanical excitation

Vertical excitation (*in vitro* tests)

Horizontal excitation (*in vivo* tests)

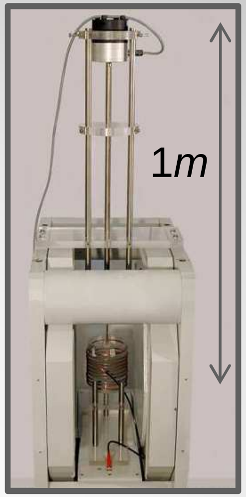

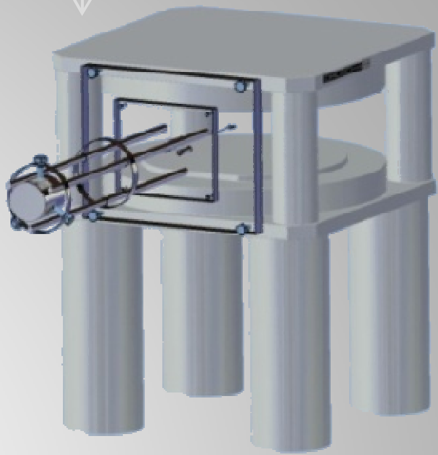

Experimental device with horizontal excitation

Experimental device with vertical excitation

Wave equation inversion 2D-algorithm

Assumption of a purely elastic medium	Assumption of a viscoelastic medium
$G = \rho . \left(\frac{\omega}{k} \right)^2$	$G' = \rho \omega^2 \frac{K'^2 - K''^2}{\left(K'^2 + K''^2 \right)^2}$
ρ : *density* k : *wavenumber* ω : *frequency* λ : *wavelength*	$G'' = \rho \omega^2 \frac{K' K''}{\left(K'^2 + K''^2 \right)^2}$

In vitro tests : Validation on soft homogeneous gels

Vertical MRE Experimental device for echographic gel

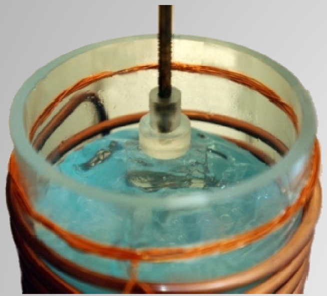

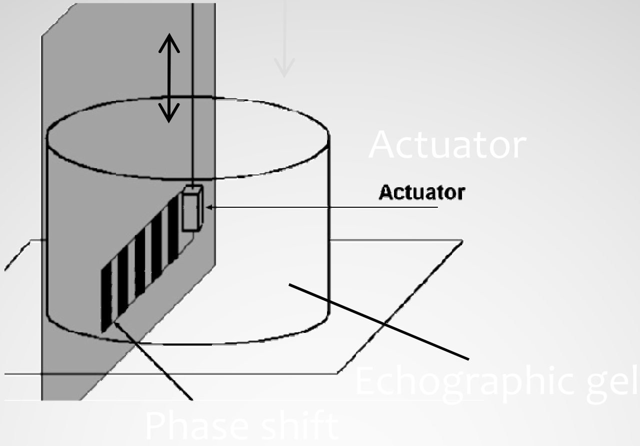

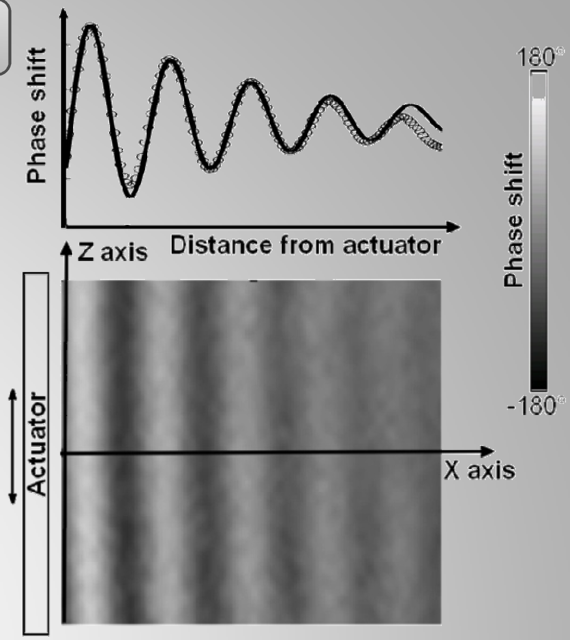

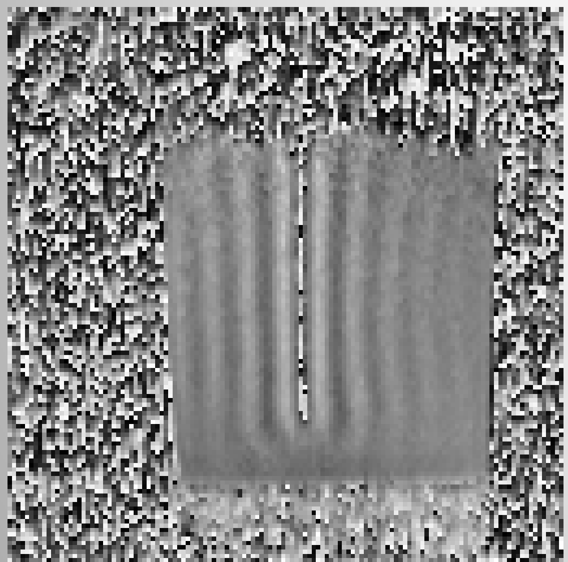

Shear wave propagation on echographic gel

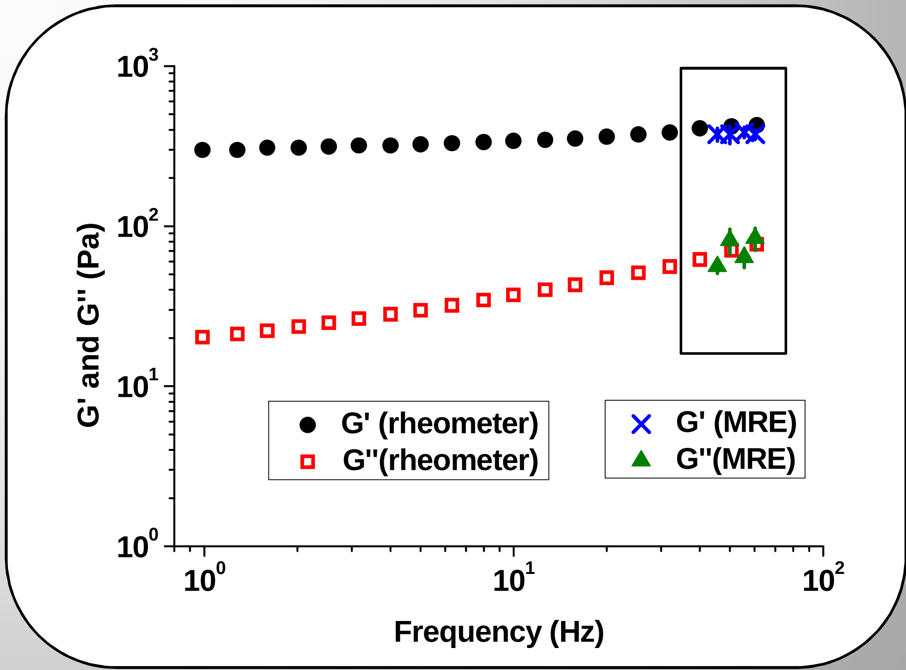

Magnetic Resonance Elastography (MRE)

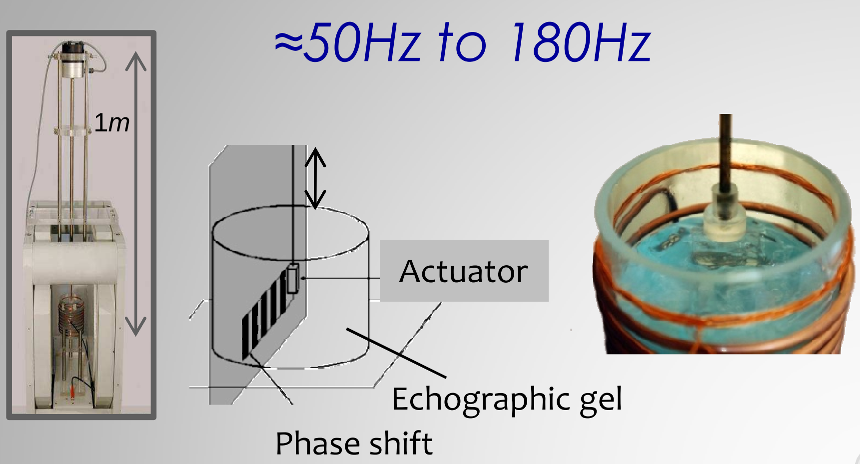

Dynamic MRI

[Vappou et al. 2007]

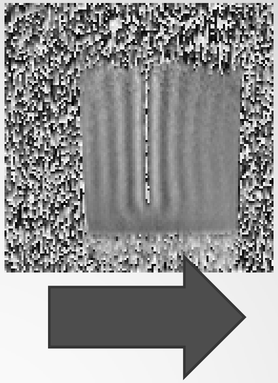

Wave propagation inverse equations

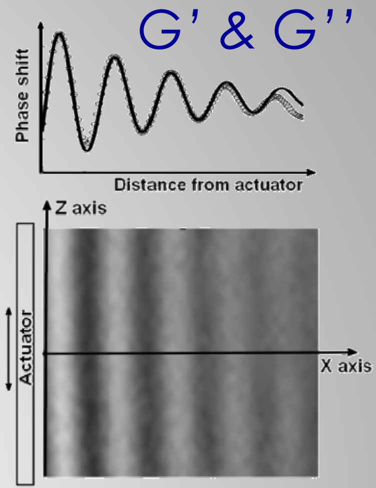

MRE

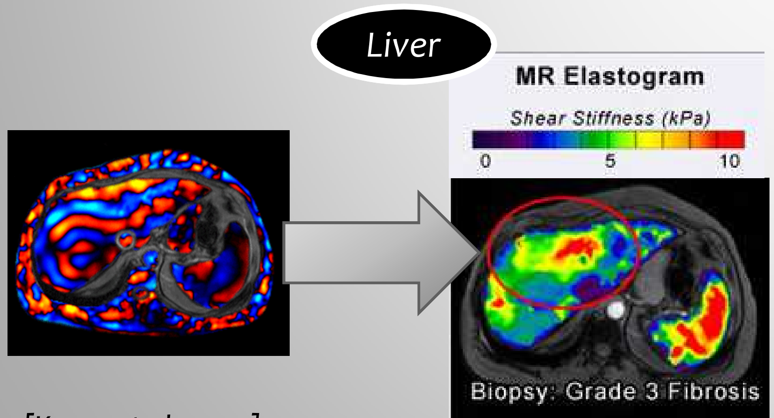

[Kruse et al. 2000]

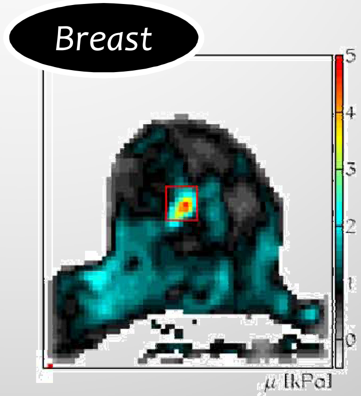

[Sinkus et al. 2005]

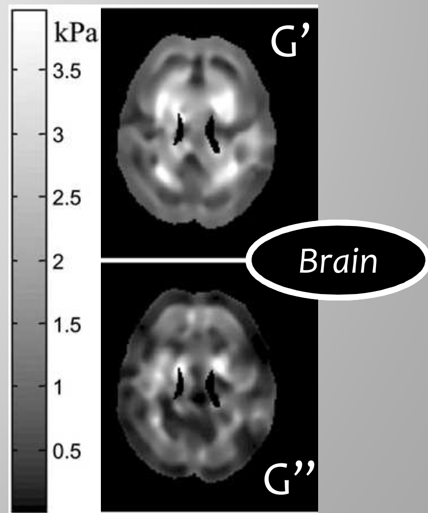

[Sack et al. 2009]

Elastographie Impulsionnelle

Transient Elastography (TE)

- *In vivo* and *ex vivo* Transient Elastography
- *Frequency: 50Hz*
- Linearity

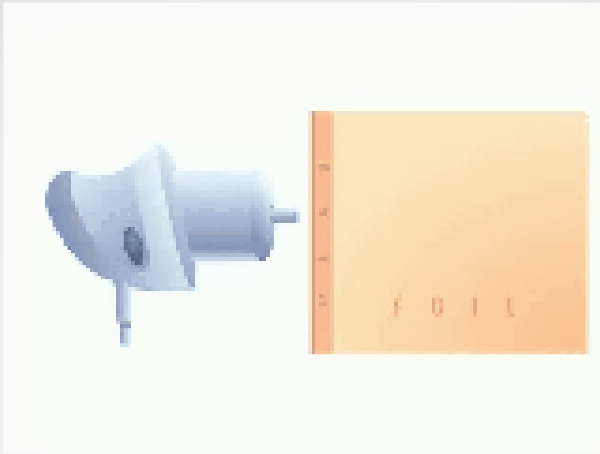

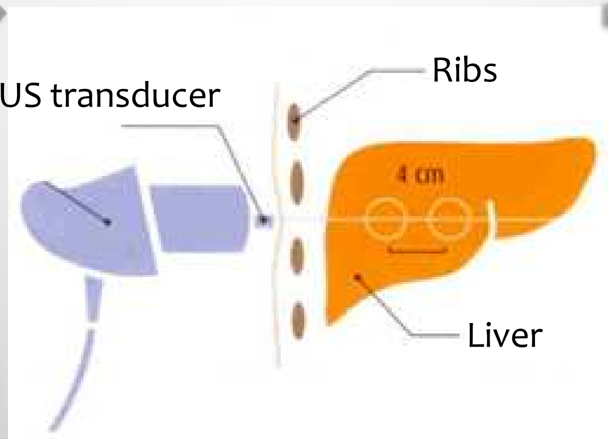

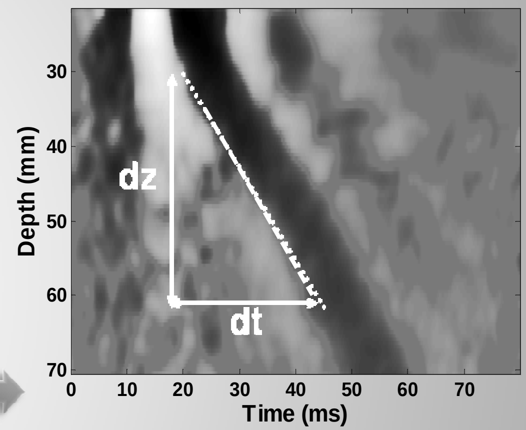

$$G = \rho V_s^2 = \rho \left(\frac{dz}{dt} \right)^2$$

Fibroscan (Echosens, Paris, France)

L'élastographie impulsionnelle : Le Fibroscan

Fréquence de travail : 50 Hz

Hypothèses de travail : foie élastique, isotrope, li

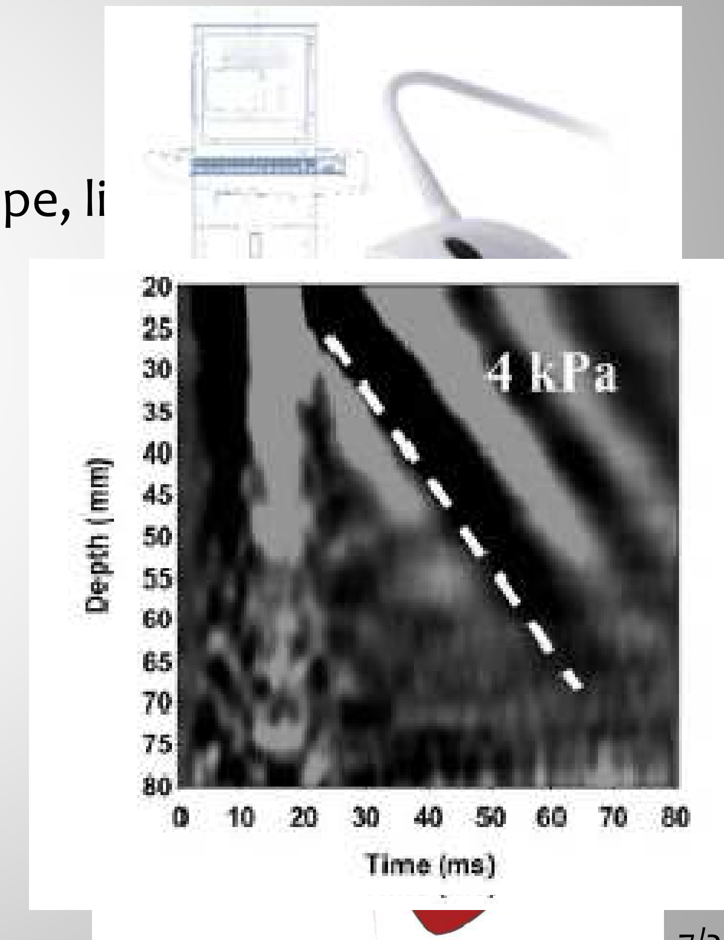

$$E = 3\rho V_S^2$$

$$\rho = 1\,\mathrm{g.cm^{-3}}$$

Vs — Vitesse de propagation de l'onde de cisaillement

Matière hépatique

ETUDE BIBLIOGRAPHIQUE

Les méthodes de caractérisation des propriétés mécaniques des tissus mous de la littérature (liste non exhaustive)

Auteur	Année	Méthode	Organe	Conditions	Type d'individu	Fréquence (Hz)	E (kPa)	G (kPa)
Brown	2003	ultrason	foie	in vivo	porc	1	80	
Chen	1996	ultrason	foie	in vitro	bovin	-	0,62 +/- 0,24	
Klatt	2006	MRE	foie	in vivo	homme malade	50 - 80		3 +/- 0,24
Kruse	2000	MRE	foie	in vitro	porc	100		2,5 – 4
Kruse	2000	MRE	foie	in vitro	porc	300		4 – 6,2
Carter	2001	indentation	foie	in vivo	homme sain	statique	270	
Carter	2001	indentation	foie	in vivo	homme malade	statique	740	
Kim	2003	indentation	foie	in vivo	porc	100	31,8	
Ottensmeyer	2001	indentation	foie	in vitro	porc	0,1 - 60	2,2	
Samur	2005	indentation	foie	in vitro	porc	statique	15	

ETUDE BIBLIOGRAPHIQUE

Auteur	Tissu	Conditions	Technique	E (en kPa)	G (en kPa)
Huwart	Foie homme	In vivo	MRE	7	
Klatt	Foie homme	In vivo	MRE		2,26 +/- 0,23
Ottensmeyer	Foie homme	In vivo	indentation	2,2	
Roulot	Foie homme	In vivo	Fibroscan	5,49 +/- 1,59	

Literature review

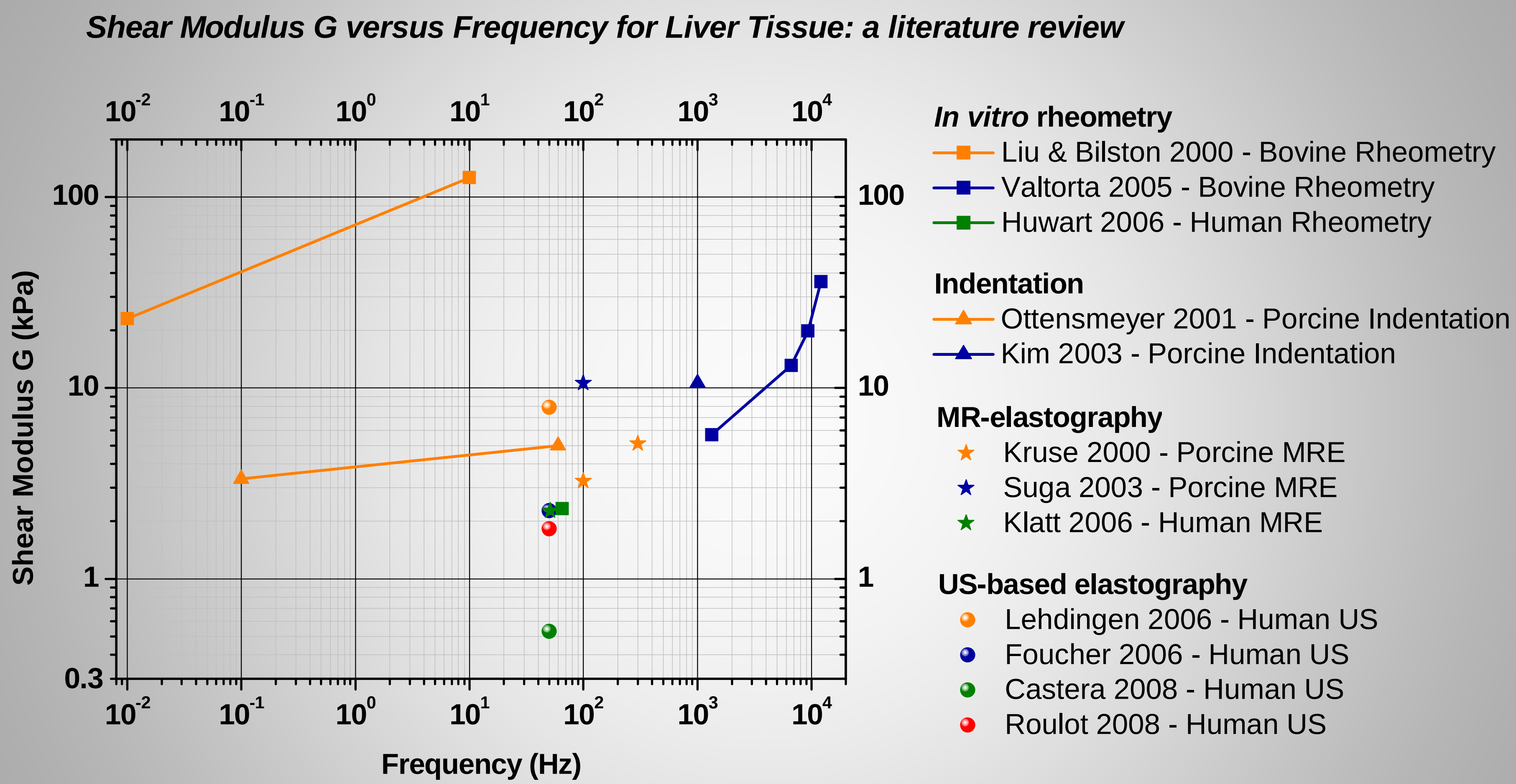

Difficulties to compare the results: inter-species variations, protocols, frequency ranges, strain rates,…

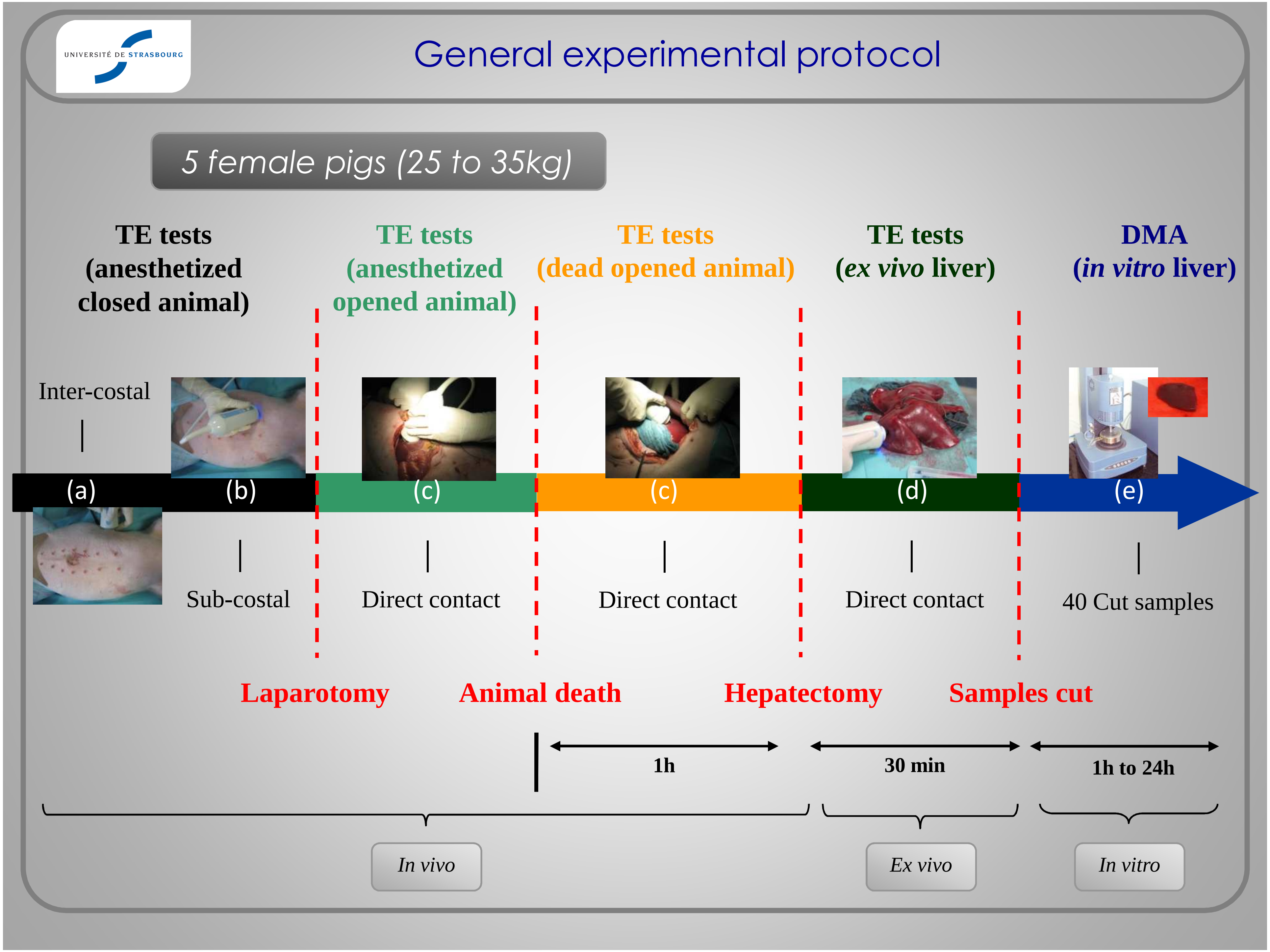

UNIVERSITÉ DE STRASBOURG
General experimental protocol
5 female pigs (25 to 35kg)
TE tests (anesthetized closed animal)
TE tests (anesthetized opened animal)
TE tests (dead opened animal)
TE tests (ex vivo liver)
DMA (in vitro liver)
Inter-costal
(a)
(b)
(c)
(c)
(d)
(e)
Sub-costal
Direct contact
Direct contact
Direct contact
40 Cut samples
Laparotomy
Animal death
Hepatectomy
Samples cut
1h
30 min
1h to 24h
In vivo
Ex vivo
In vitro

In vivo Transient Elastography tests

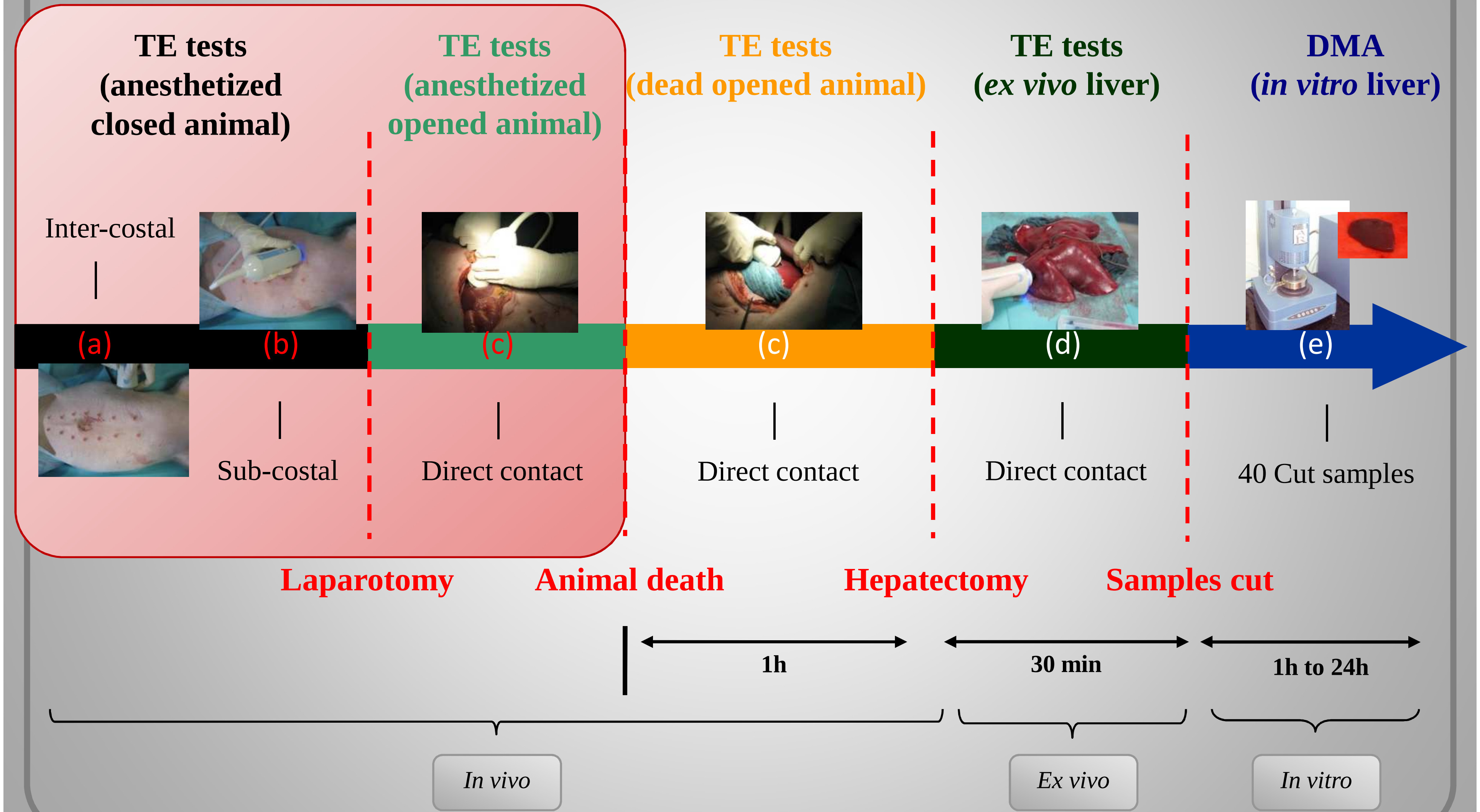

In vivo Transient Elastography tests

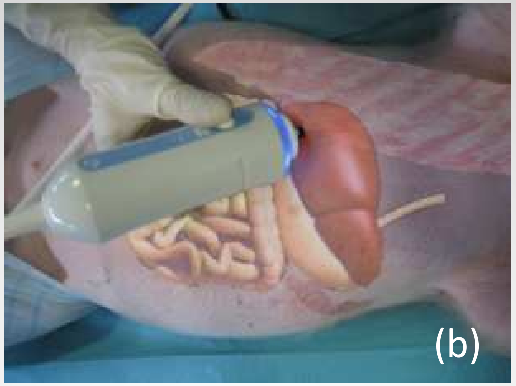

3 *in vivo* US-TE configurations:

- (a) *In vivo* inter-costal (anesthetized closed animal)
- (b) *In vivo* sub-costal (anesthetized closed animal)
- (c) *In situ* (anesthetized or dead opened animal)

For each configuration:
5 pigs
10 measurements/pig

→ *1 mean shear modulus value*

In vivo Transient Elastography results

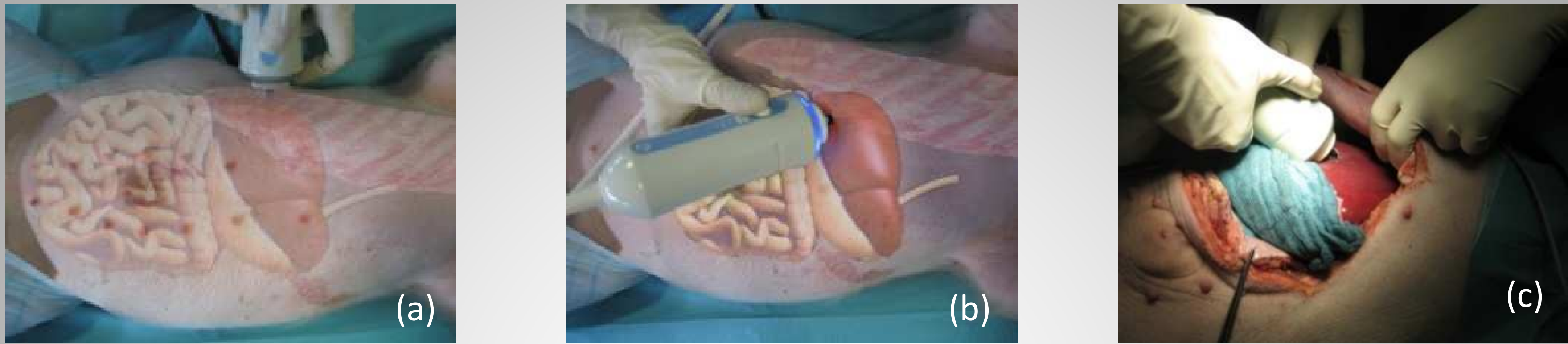

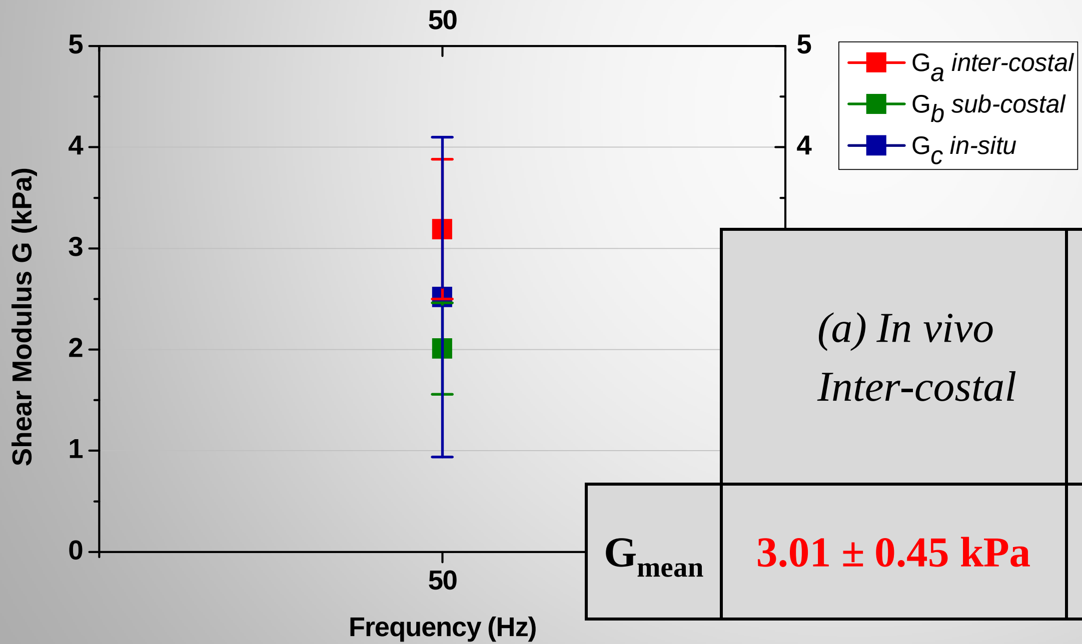

	(a) In vivo Inter-costal	*(b) In vivo Sub-costal*	*(c) In situ*
G_{mean}	**3.01 ± 0.45 kPa**	**3.19 ± 0.69 kPa**	**2.52 ± 1.58 kPa**

Ex vivo TE & DMA tests

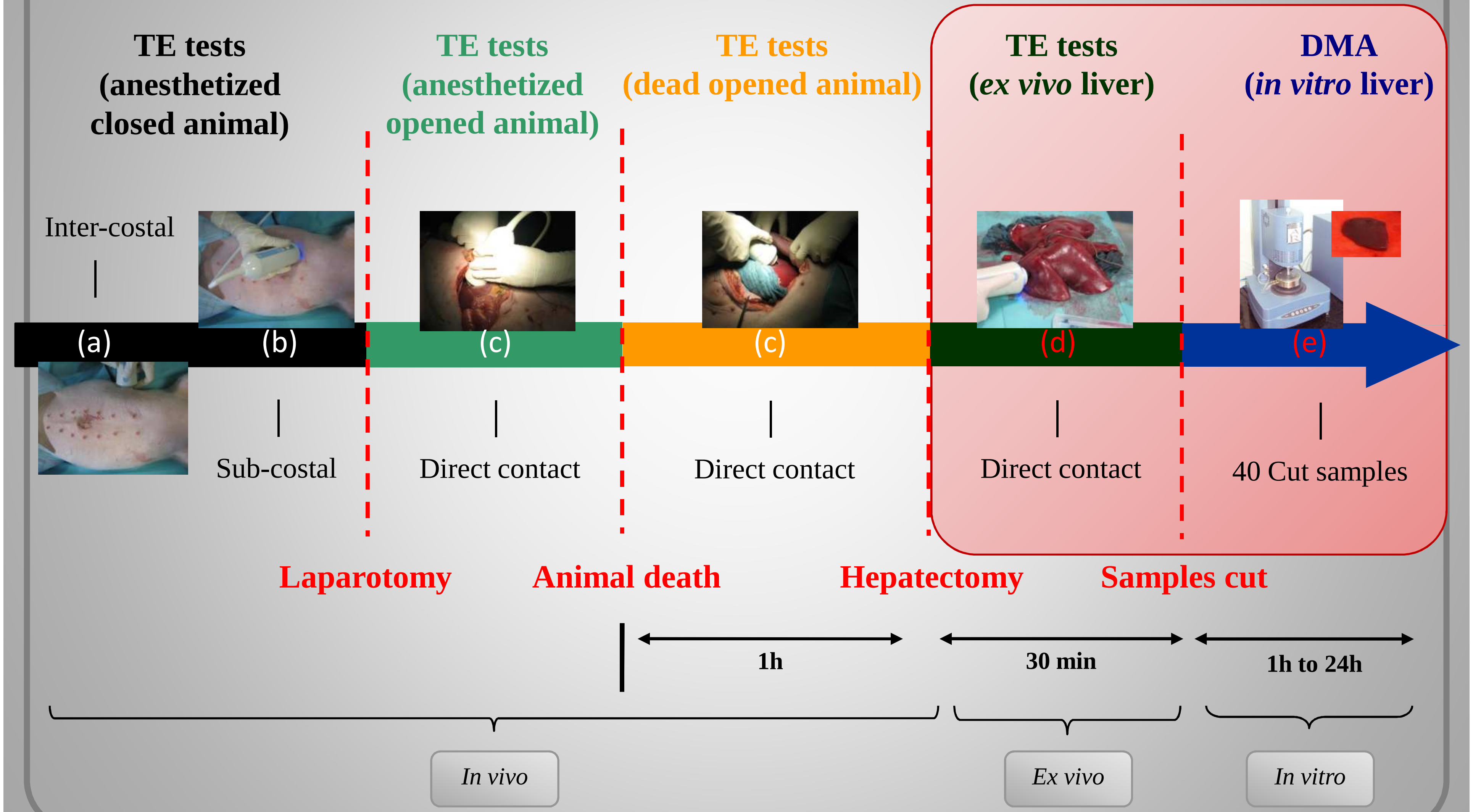

Ex vivo Transient Elastography tests

Ex vivo US-TE configuration (d):

- *Ex vivo*

(dead animal after hepatectomy)

- Clamped liver:

  maintained blood pressure

- Controlled temperature

In vitro DMA tests (e):

- *Ex vivo*
- Clamped liver:

  maintained blood pressure

- Temperature monitoring

Ex vivo results: TE versus DMA

Mean storage G' (square) and loss G'' (triangle) moduli obtained by Dynamic Mechanical Analysis on *in vitro*porcine hepatic tissue samples

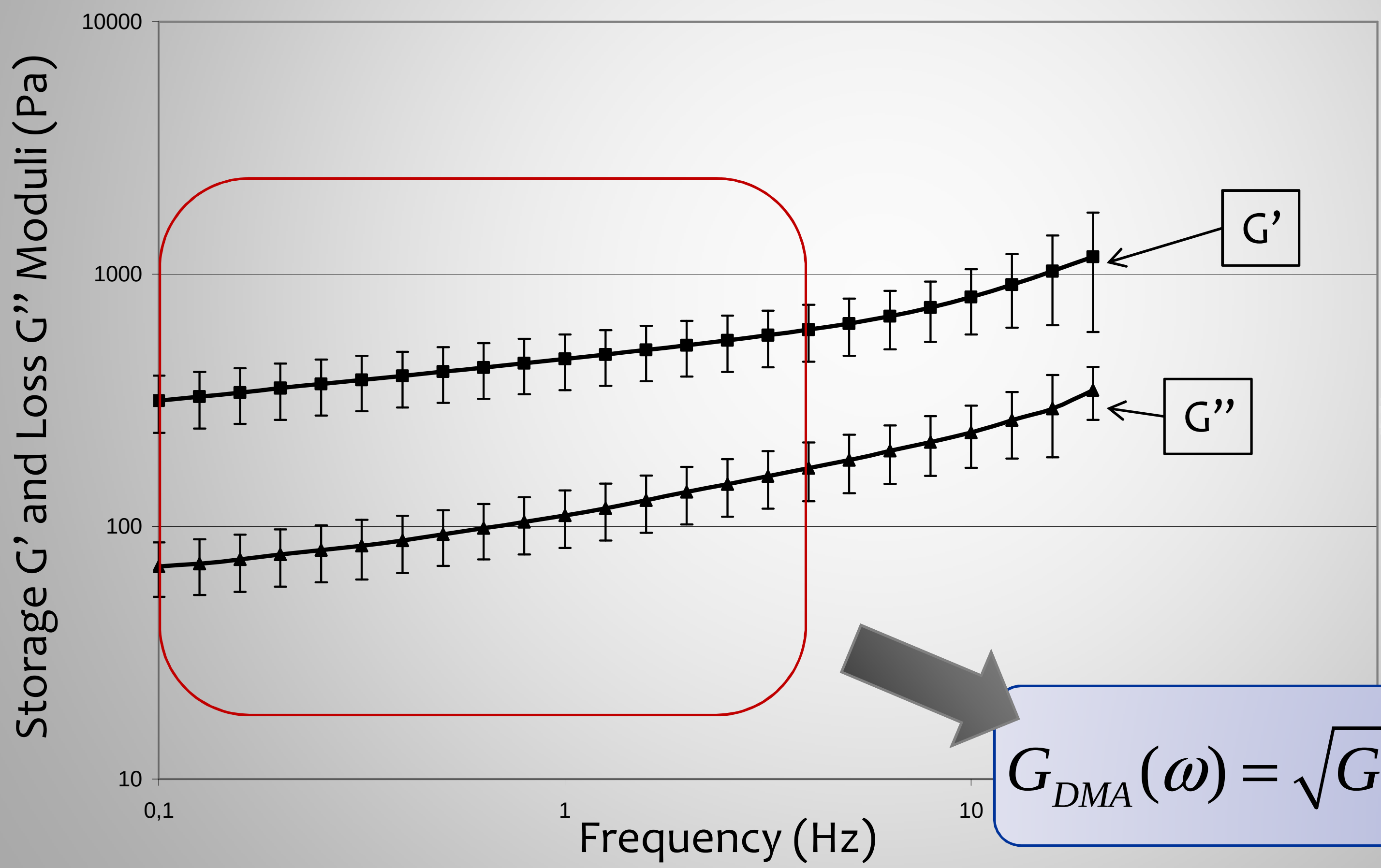

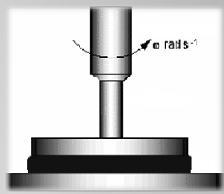

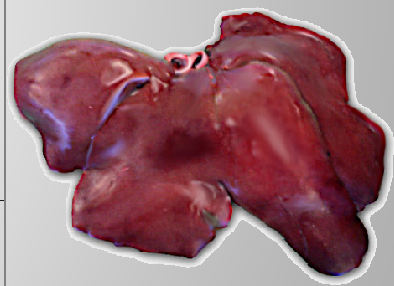

$$G_{DMA}(\omega) = \sqrt{G'(\omega)^2 + G''(\omega)^2}$$

Ex vivo results: TE versus DMA

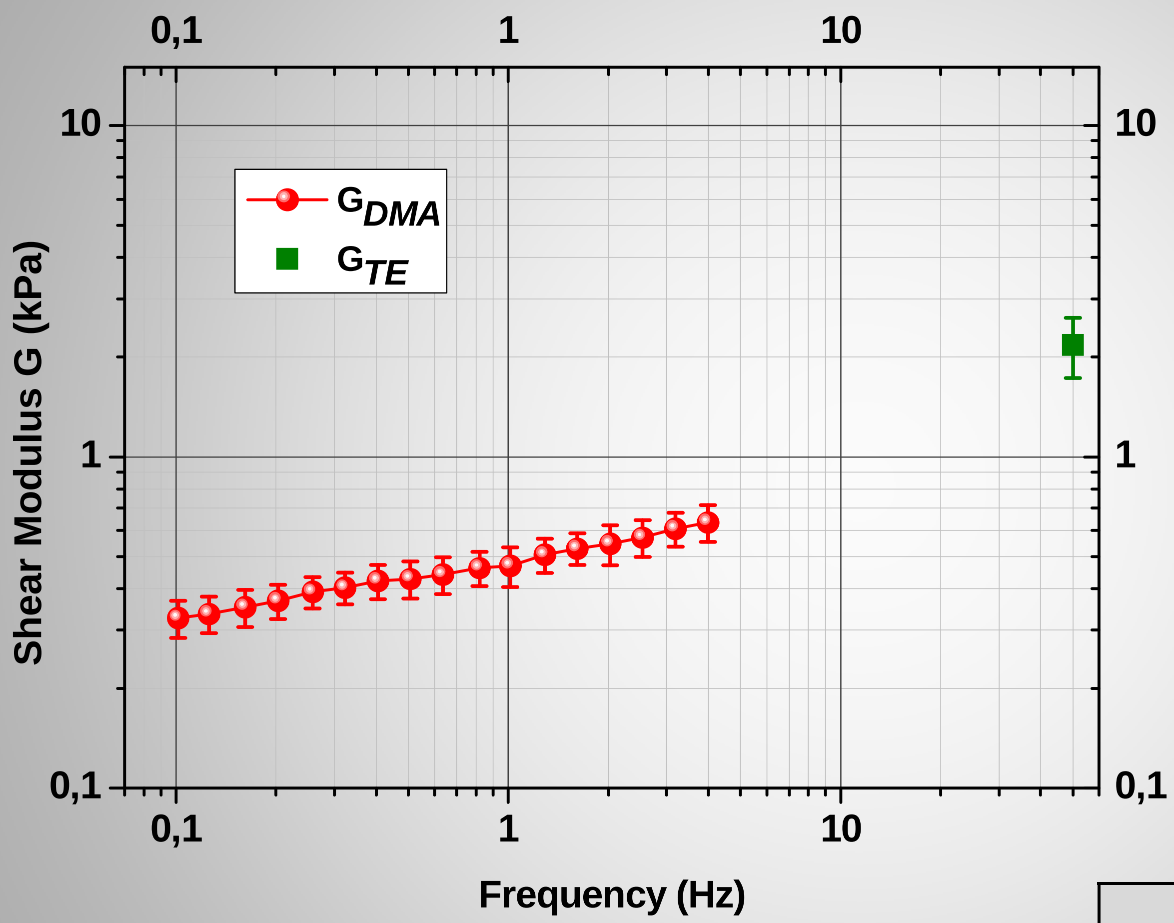

5 porcine livers
-
40 DMA samples
50 TE tests

	(d) Ex vivo TE
G_{mean}	**2.18 ± 0.45 kPa**

Ex vivo results: TE versus DMA

Shear Modulus G versus Frequency for Liver Tissue: comparison with the results from the literature

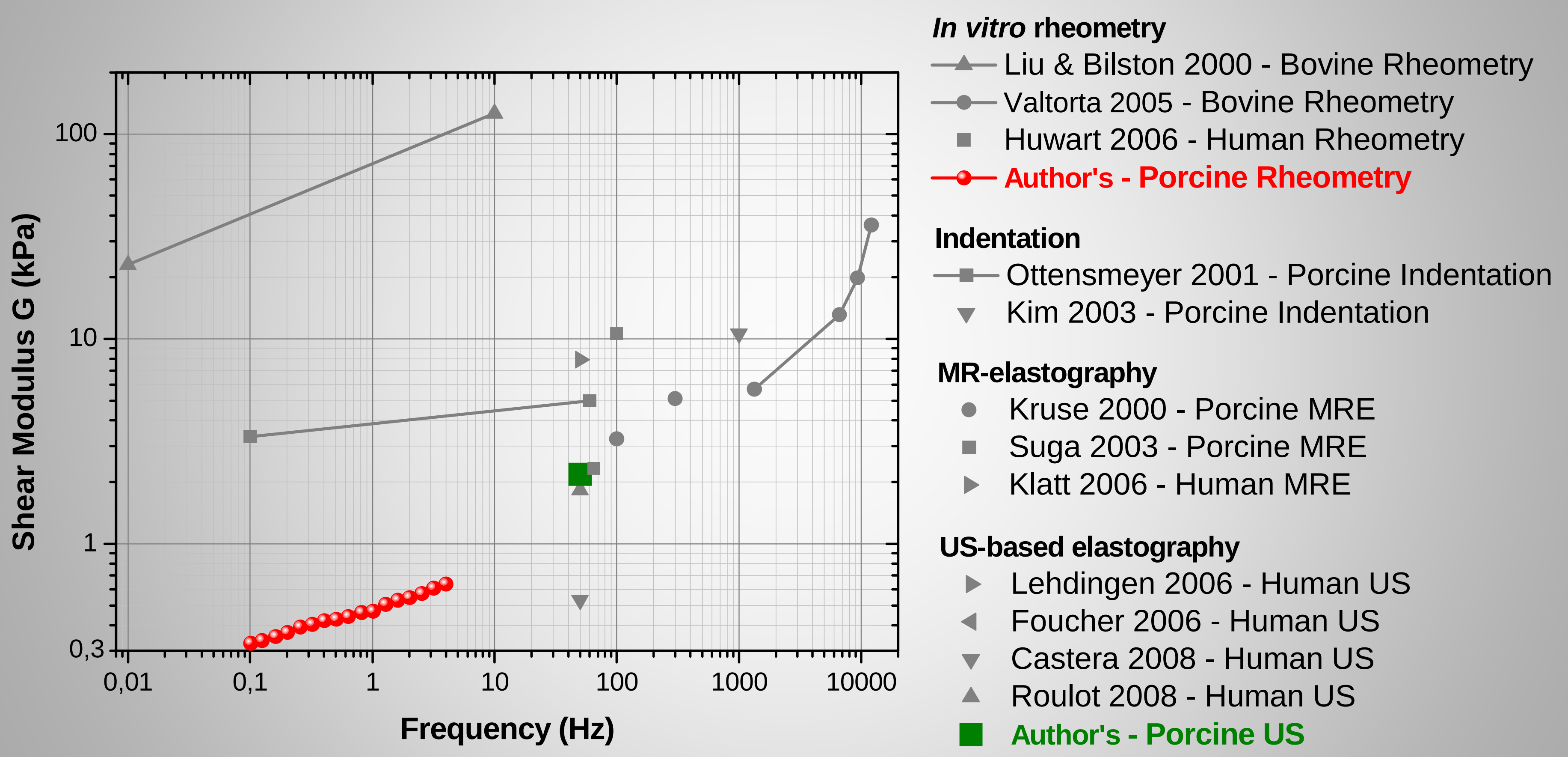

US-TE validated

Analyse in vitro et modélisation

Ex vivo Hepatic tissue properties

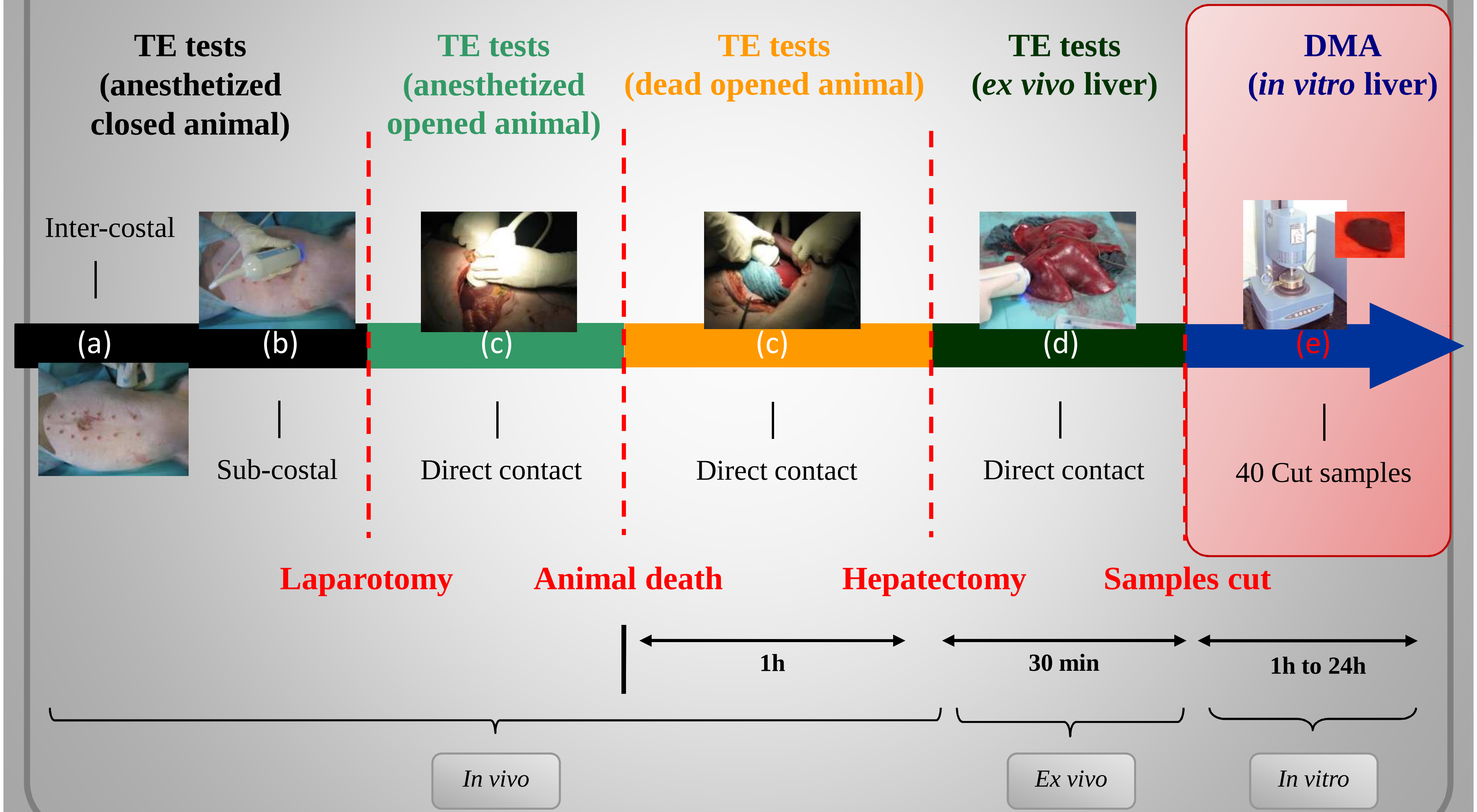

In vitro liver anisotropy investigation

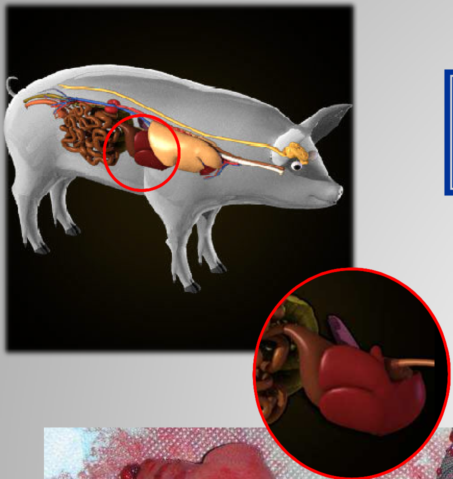

Porcine liver

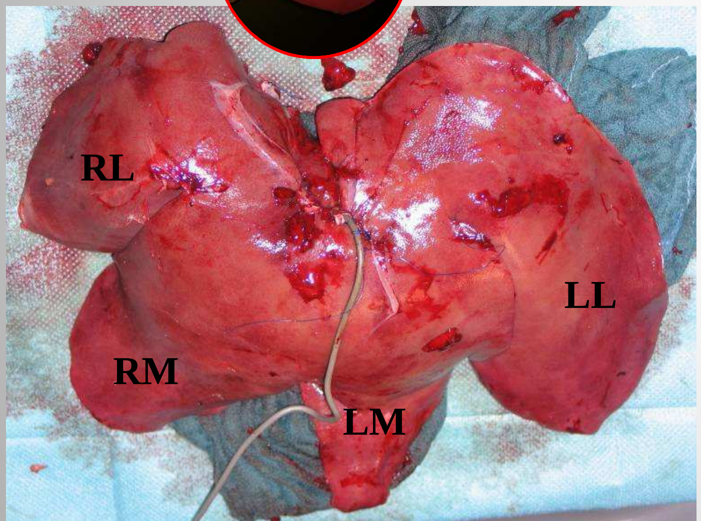

RL: right lateral lobe

RM: right median lobe

LM: left median lobe

LL: left lateral lobe

Human liver

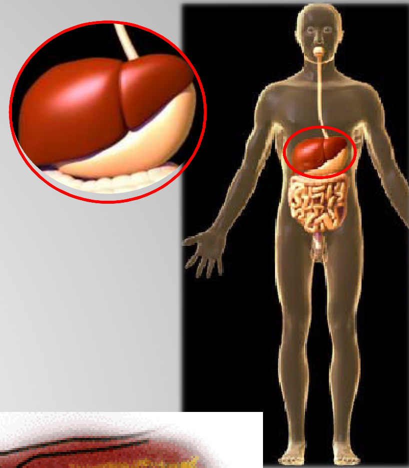

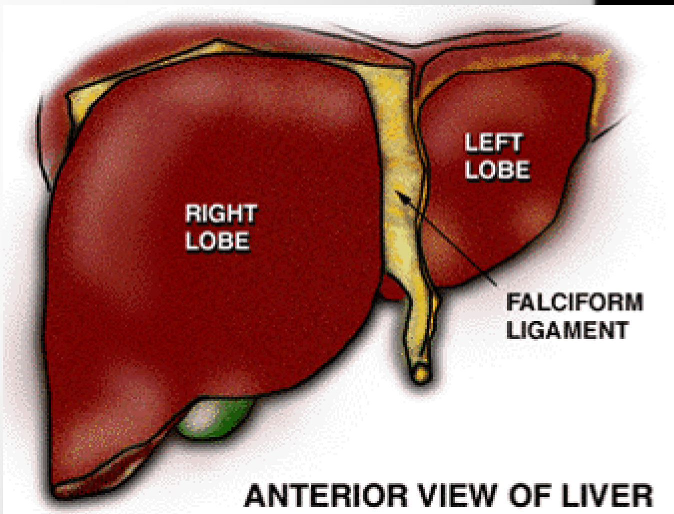

In vitro liver anisotropy investigation

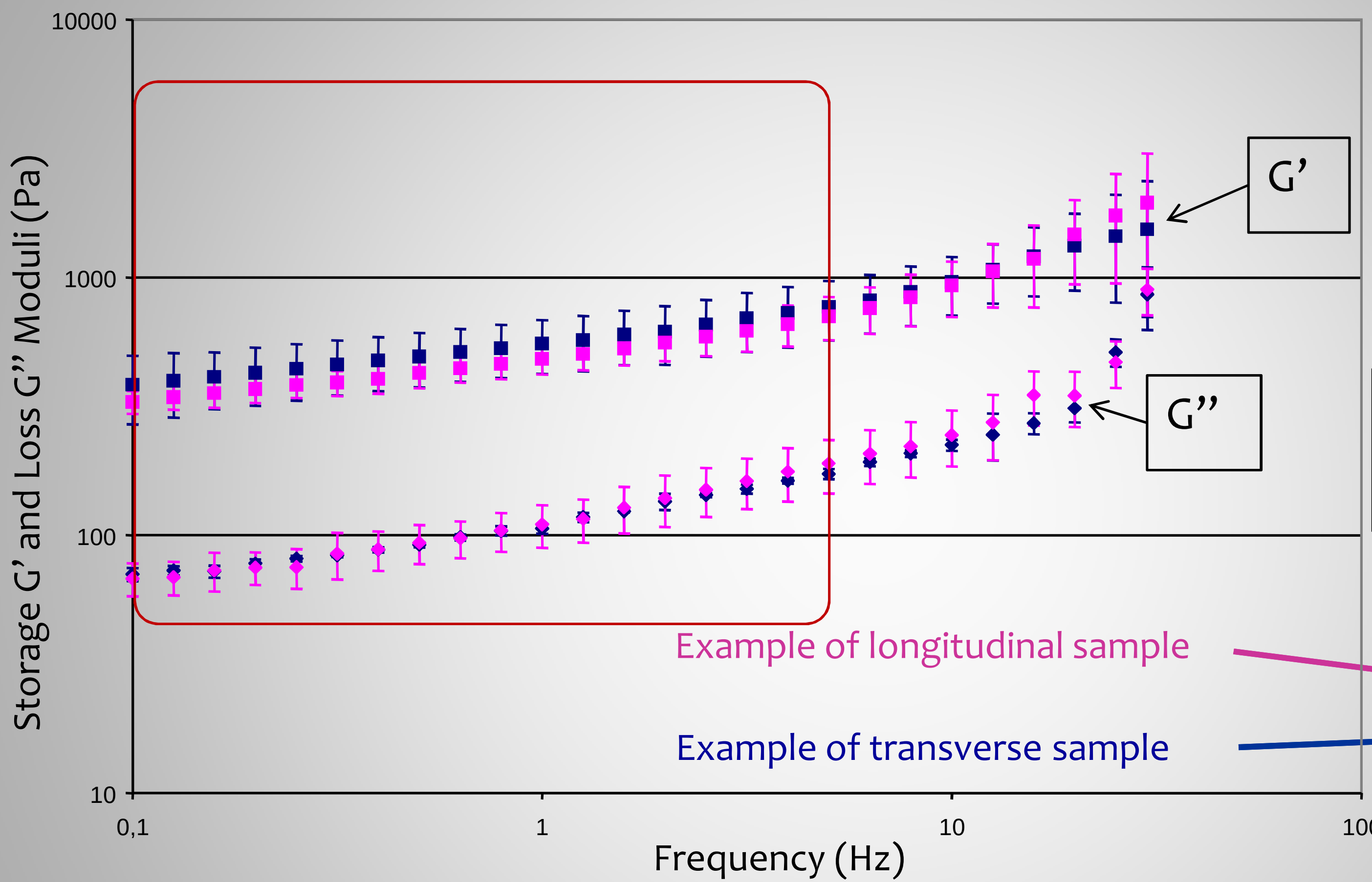

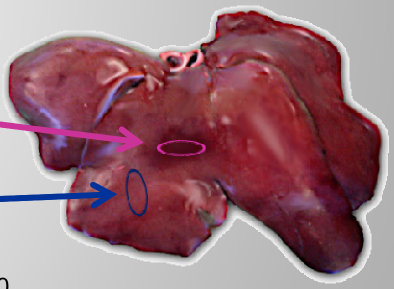

No significant hepatic tissue anisotropy influence

In vitro liver heterogeneity investigation

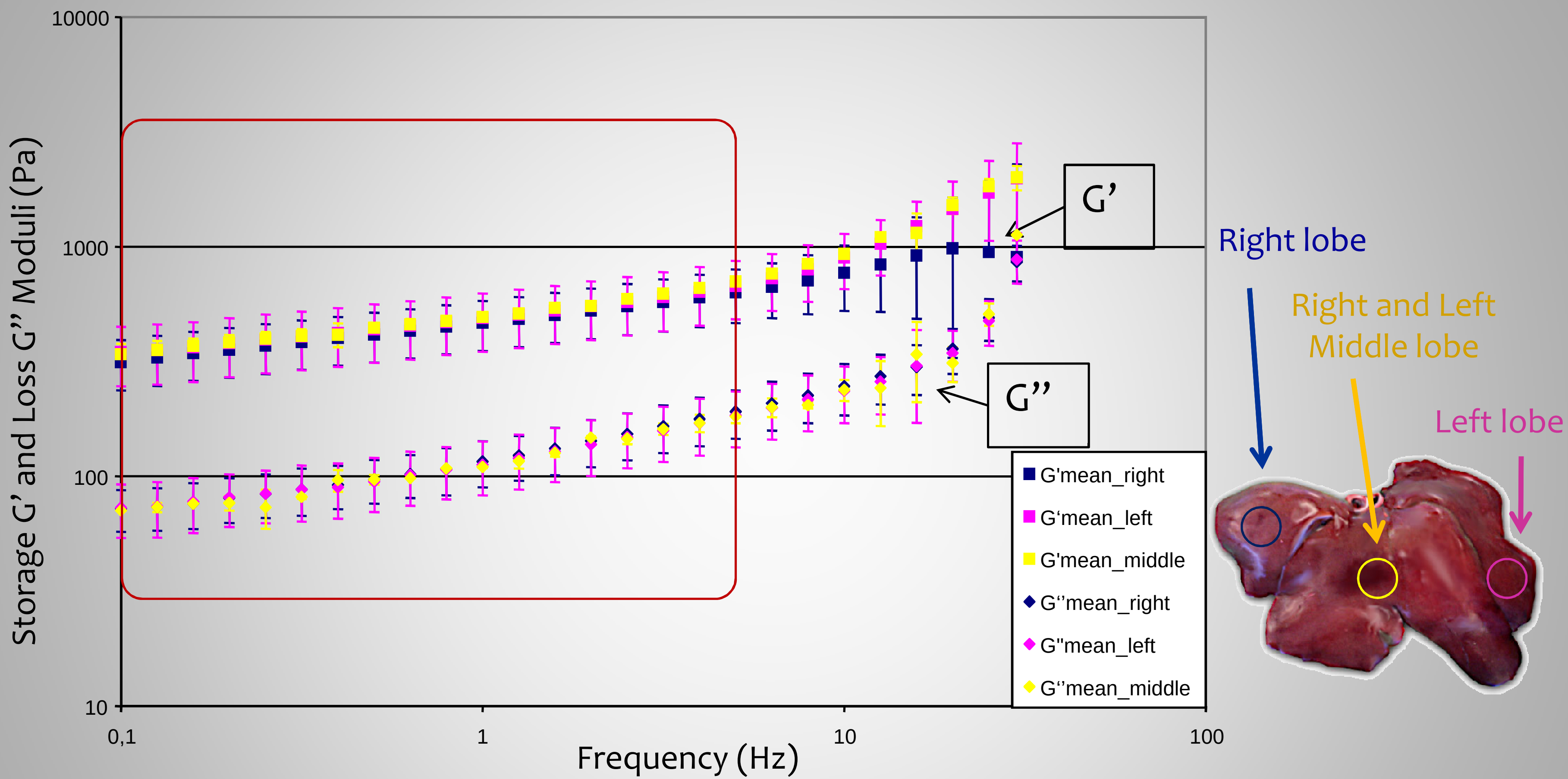

No significant hepatic tissue heterogeneity influence

Post mortem time influence

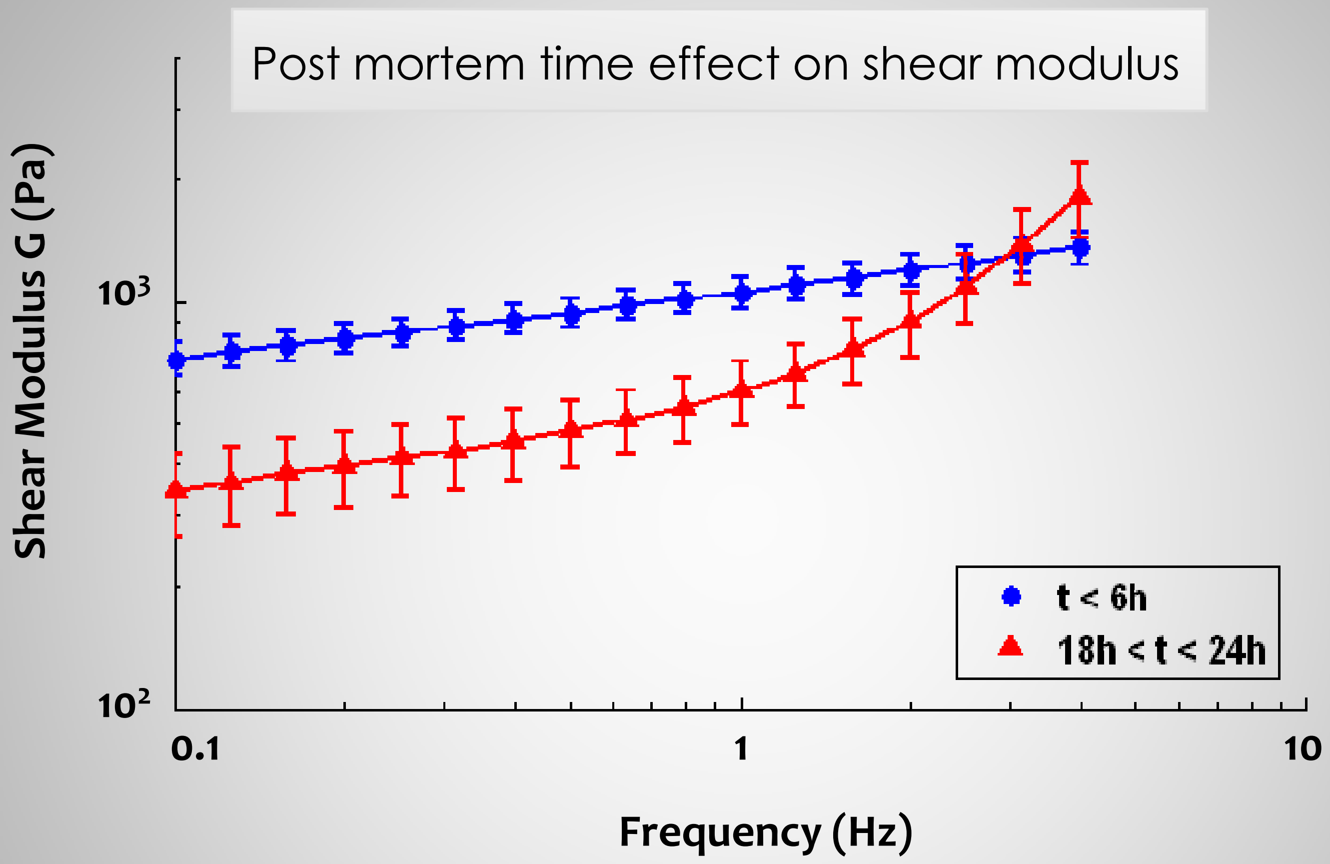

***Post mortem* time effect on the linear viscoelastic strain limit**	**Short time: γ_{lim}**	0.8 ± 0.3 - 1.8 ± 0.2
	Long time: γ_{lim}	5.6 ± 2.4 - 6.3 ± 0.0

Hepatic tissue modeling

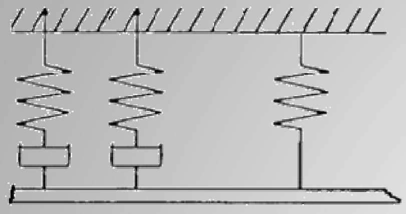

Generalized Maxwell model

- 2 relaxation modes
- Based on 0.1 to 10Hz DMA mean results

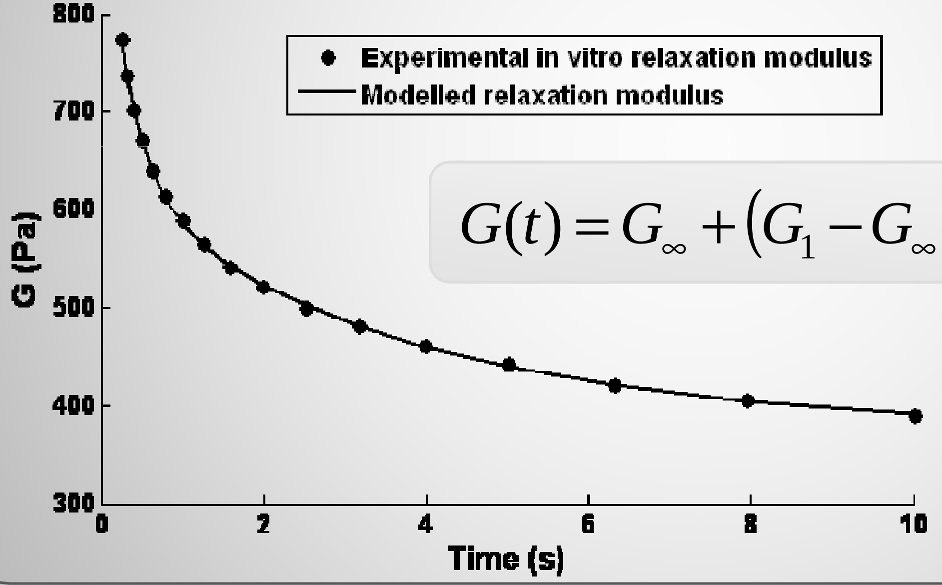

$$G(t) = G_\infty + (G_1 - G_\infty)e^{-\beta_1 t} + (G_2 - G_\infty)e^{-\beta_2 t}$$

G_∞ (Pa)	G_1(Pa)	β_1 (s^{-1})	G_2(Pa)	β_2(s^{-1})
377	169	1	290	10

Conclusions

Conclusions

- All the tests on the same 5 porcine livers
    - 3 in vivo configurations comparison
    - *Ex vivo* US-TE / *In vitro* DMA
- Mean shear modulus value at 50Hz:
- Mean shear modulus value at 50Hz:
    - *In vivo*: G = 2.0 ± 0.5 kPa
    - *In vitro*: G = 1.2 ± 0.4 kPa
- Hepatic tissue characterization
    - Homogeneous
    - Isotropic
    - High *post mortem* time dependence

Perspectives and limits

- More significant number of animals
- Same protocol to characterize fibrosis
- No *in vivo* viscosity measurement, but elastic assumption validated

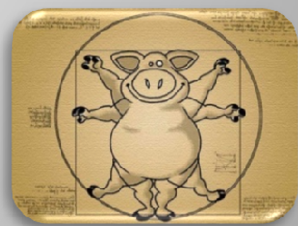

Matière Cérébrale

Modeling of Shear Linear Behavior
(Commonly used in the literature)

$G_0 - G_\infty$

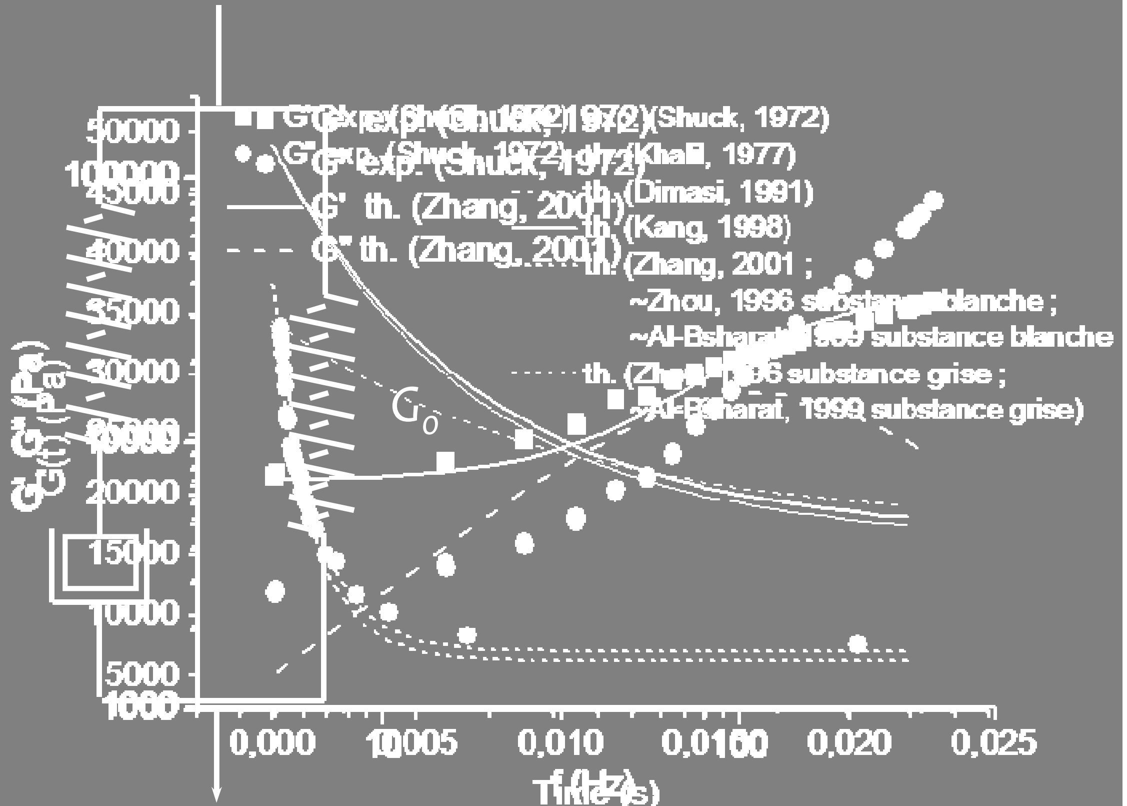

$\eta = (G_0 - G_\infty)/\beta$

Relaxation Modulus:

$$G(t) = G_\infty + (G_0 - G_\infty)\,e^{-\beta t}$$

Objectives

Enhance the Knowledge of the Shear Linear Behavior of Brain Tissue

Highlight the Effect of Experimental Conditions

Improve the Modeling of the Brain Tissue

Experimental Setups

"High Frequency Rheometer" (HFR)

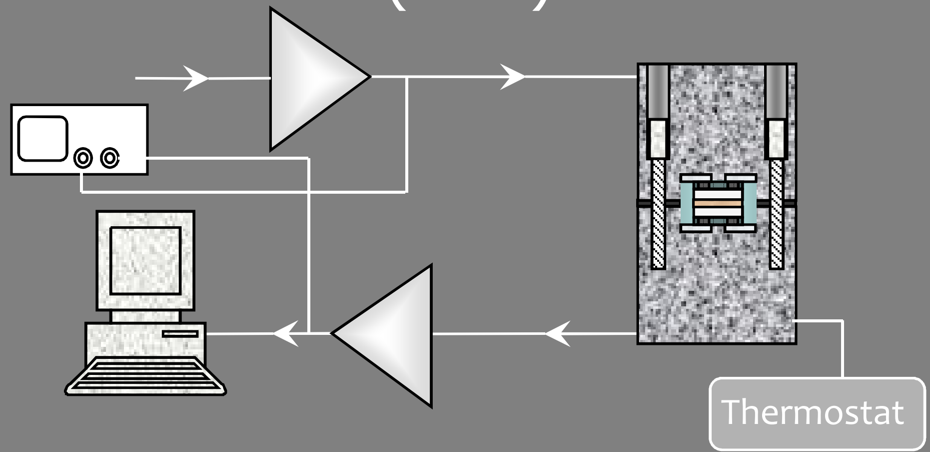

Use for translational shear tests:

- *Small strains ($Disp_{max}$ = 50 Å)*
- *Frequency sweep (f < 10 kHz)*

"Low Frequency Rheometer" (LFR)

Use for torsional shear tests:

- *Small and large strains*
- *Frequency sweep (f < 150 Hz)*
- *Time sweep (t > 0.01 s)*

Samples Origin and Preparation

Human Brain

HFR (N = 9)
White Matter
Thickness: 418 – 427 µm
Diameter: 10 mm
Sample Axis: Tr

HFR (N = 2)
Gray Matter
Thickness: 418 – 427 µm
Diameter: 10 mm
Sample Axis: Tr

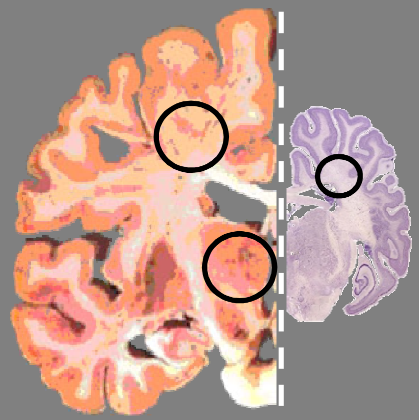

Pig Brain

(N = 21) HFR
White Matter
Thickness: 150 – 850 µm
Diameter: 10 mm
Sample Axis: Tr, A-P, S-I

(N = 7) LFR
White Matter
Thickness: 2250 µm
Diameter: 20 mm
Sample Axis: Tr

Sequence of the Tests

Experimental Condition Effects

Comparison Between

Inter-Regional Comparison

Linear Viscoelastic Limit

- Slipping Effect
- Degeneracy Effect
- Frequency Domain
- Anisotropy Effect
- Time Domain
- Human Brain
- Strain Effect

Experimental Results: Linear Domain

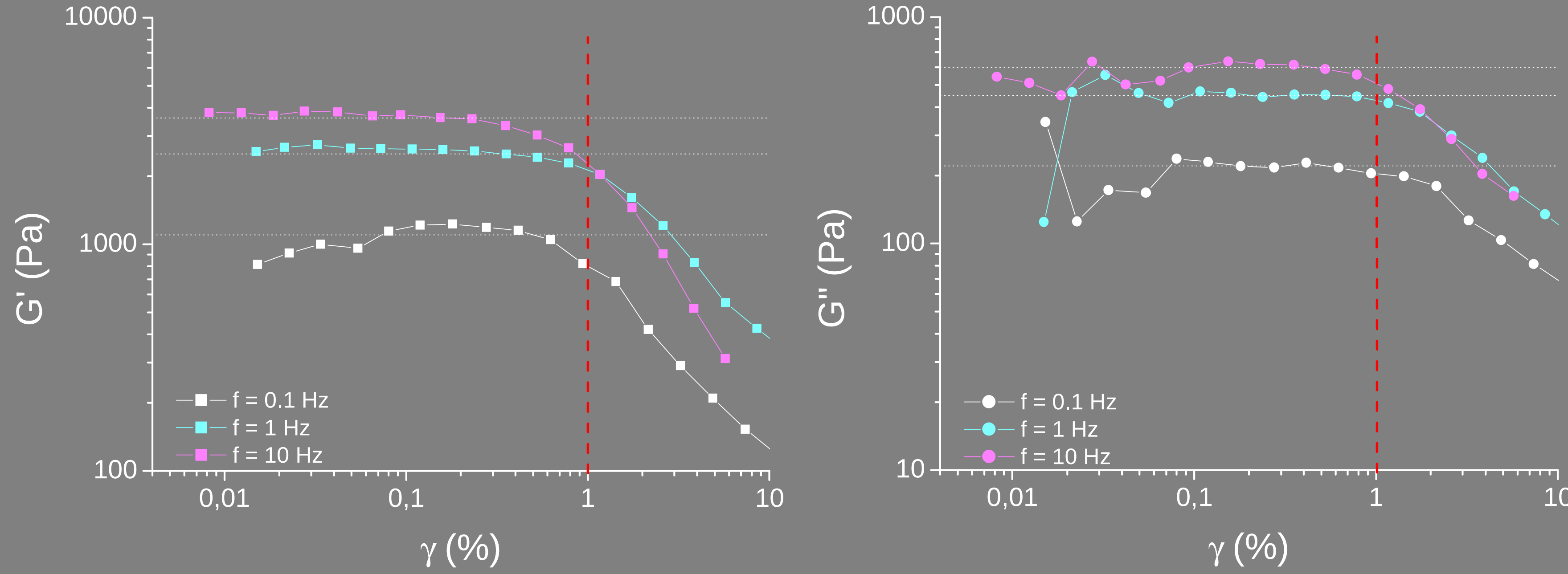

Linear Viscoelastic Limit: ~1%

Introduction | Experimental Protocol | **Linear Characterization** | Strain-Dependant Behavior

Experimental Results: Frequency Domain

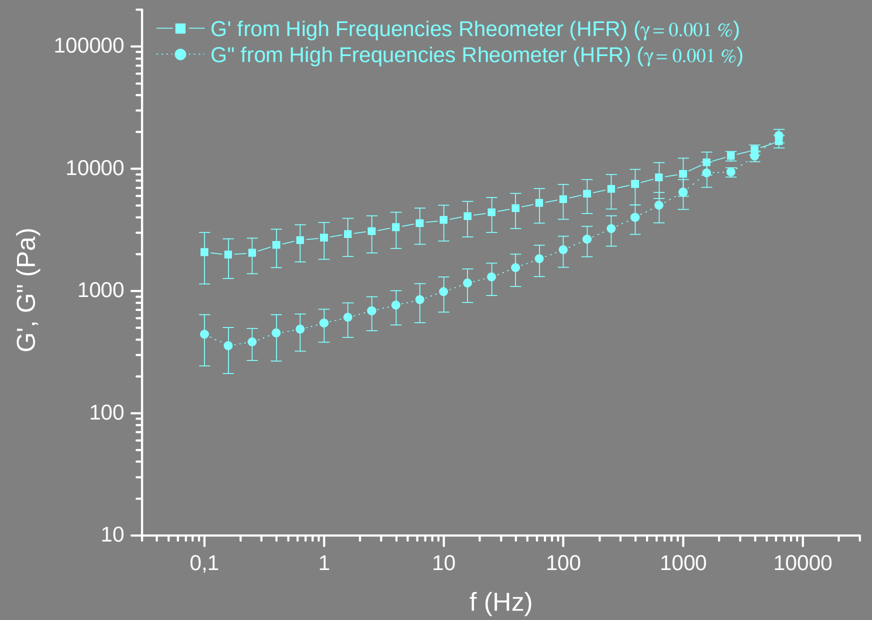

HFR Results
(N = 18)

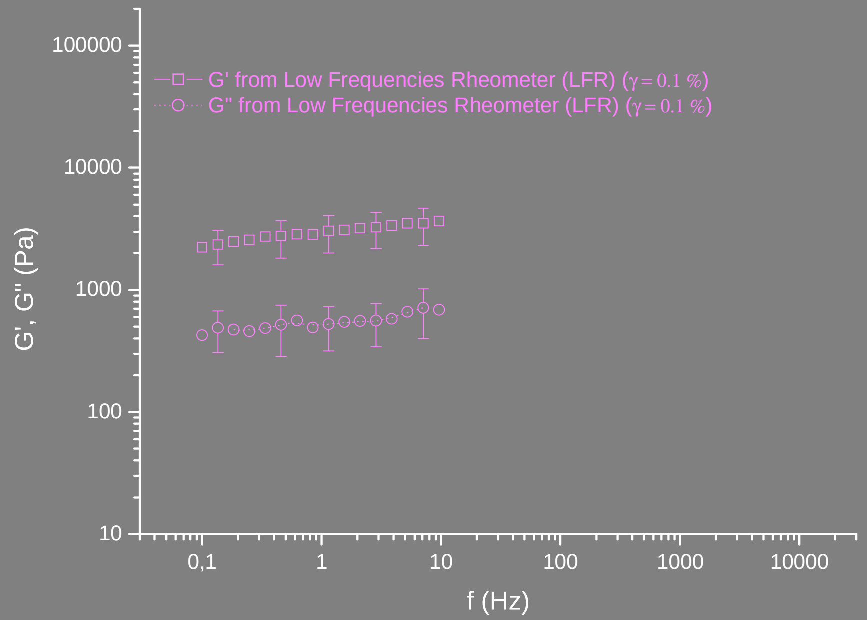

LFR Results
(N = 3)

Experimental Results: Time Domain

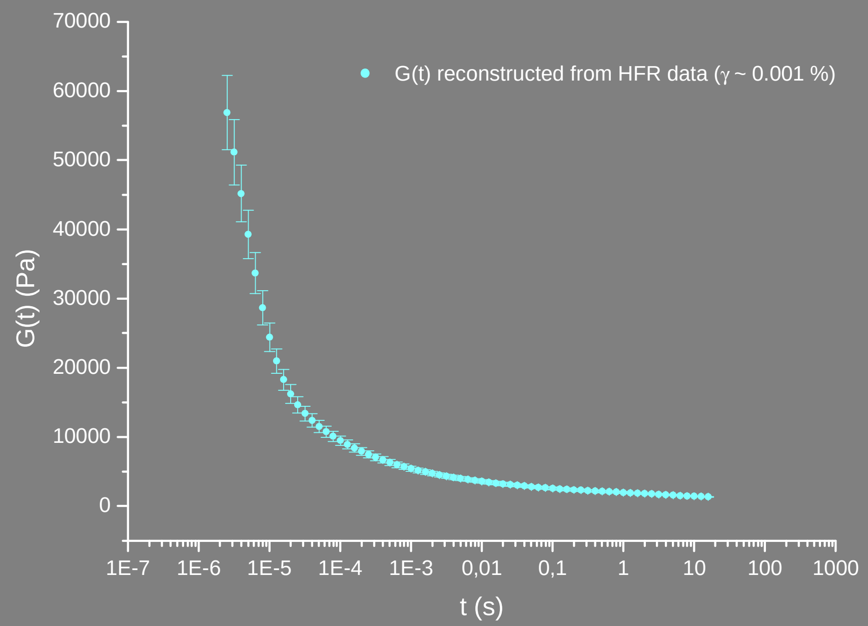

HFR Results (N = 18)

$(G',G'')_{exp}$ ⇨ $H(\tau)$ ⇨ $G(t)$

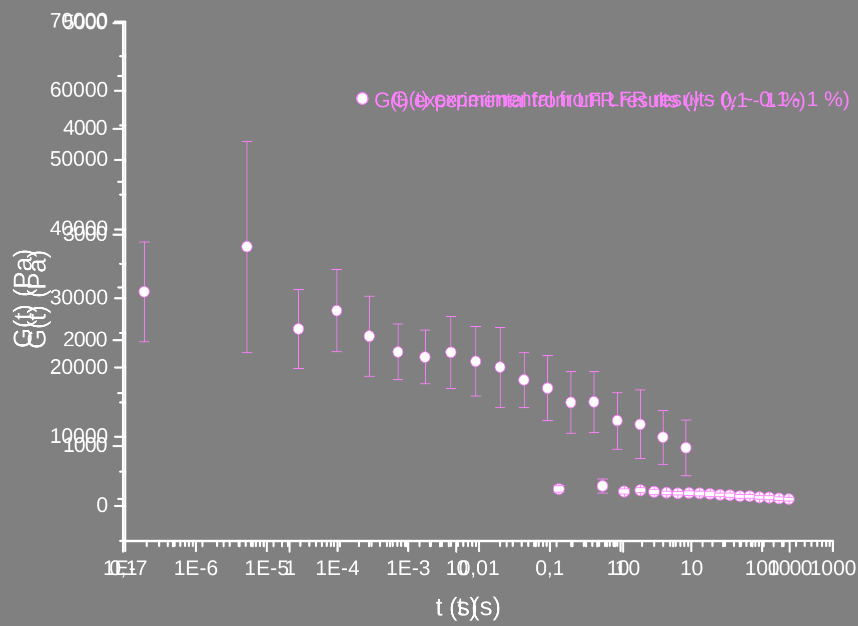

LFR Results (N = 3)

$G(t)_{exp}$

Experimental Results: Inter-Species

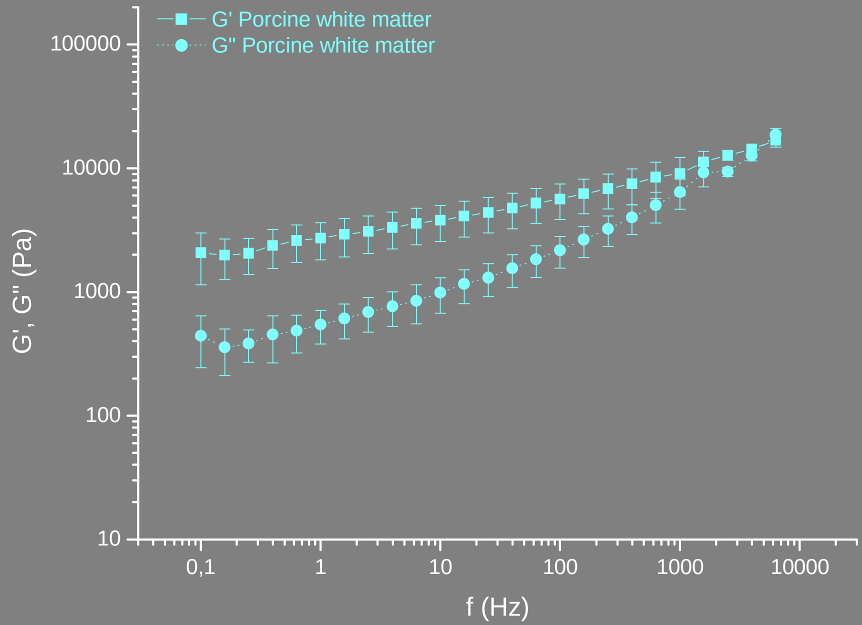

Porcine white matter
(N = 18)

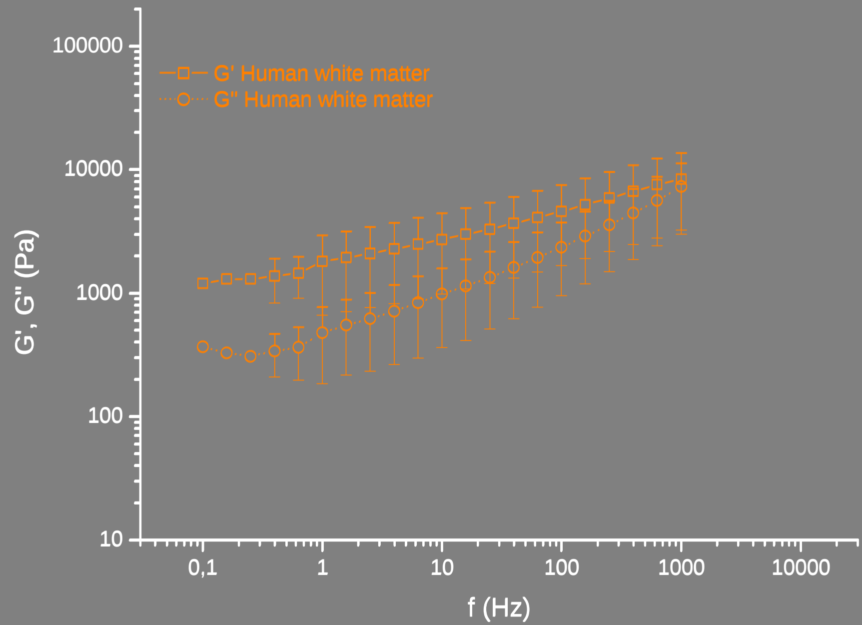

Human white matter
(N = 9)

Experimental Results: Inter-Region

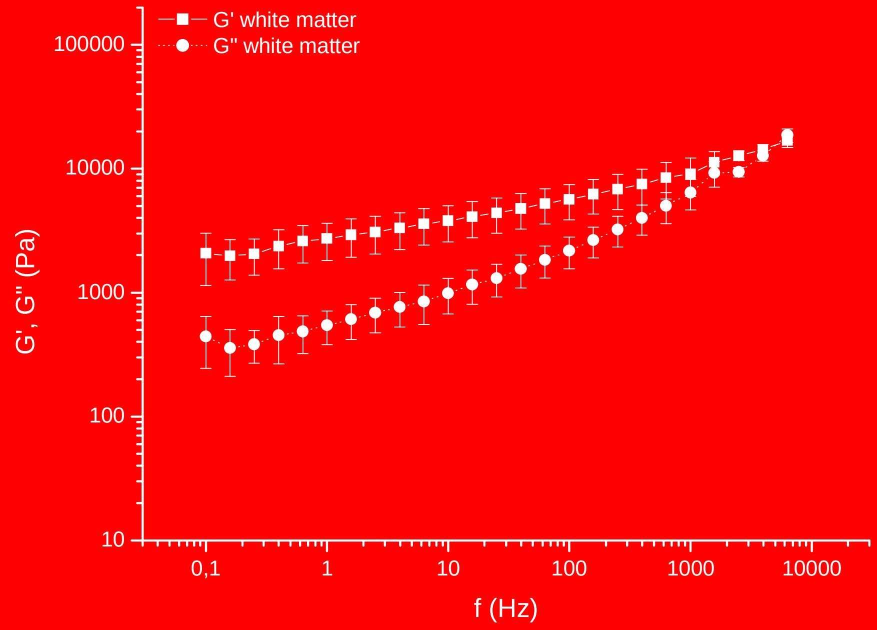

White Matter (N = 9)
(*Corona Radiata*)

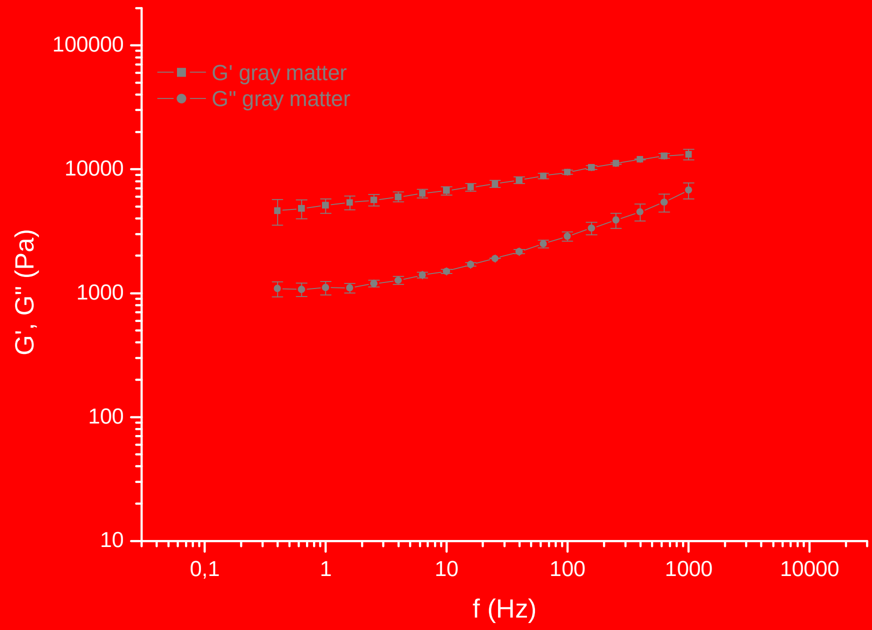

Gray Matter (N = 2)
(*Thalamic Nuclei*)

Experimental Results: Comparison with Literature

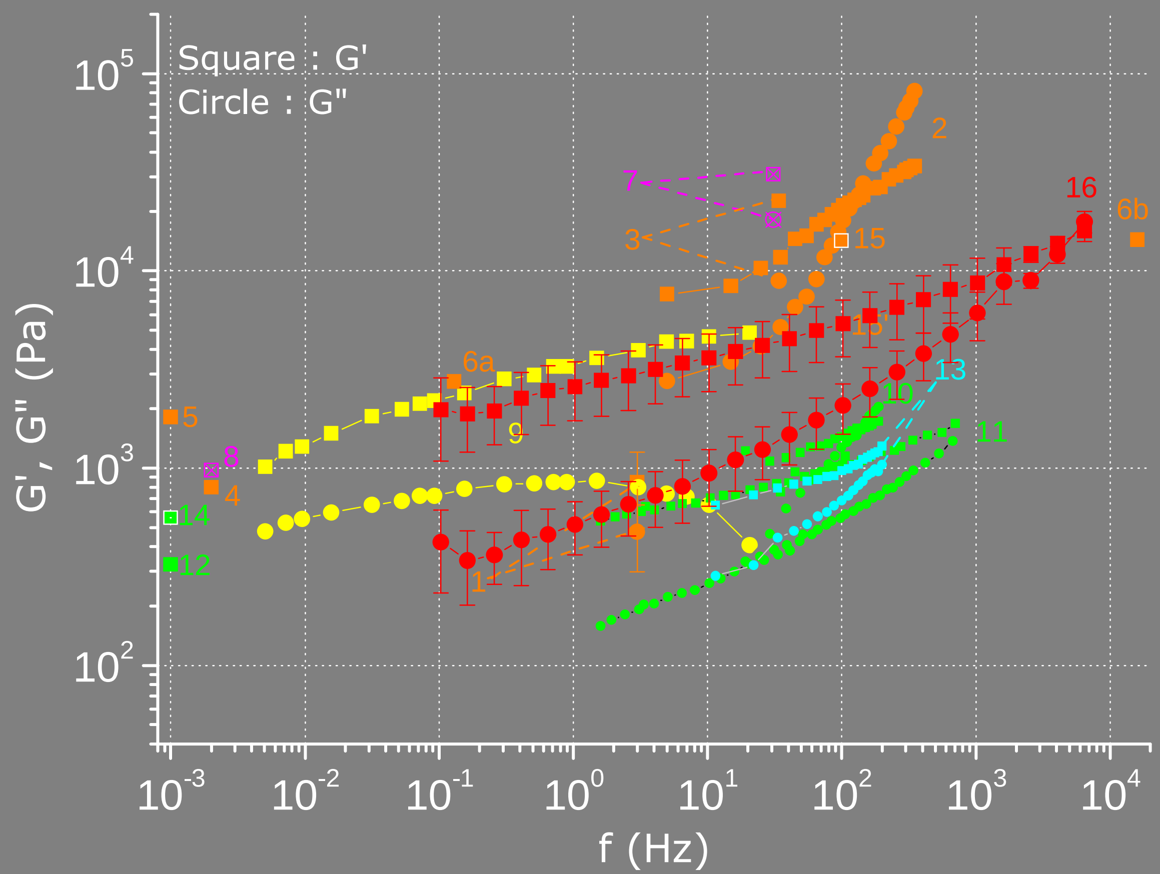

1. Human (Fallenstein, 1969)
2. Human (Shuck, 1972)
3. Human (Galford, 1970)
4. Human (Galford, 1970)
5. Human (Donnelly, 1997)
6. Human (Mendis, 1995)
7. Monkey (Galford, 1970)
8. Monkey (Galford, 1970)
9. Bovine (Bilston, 1997)
10. Porcine (Arbogast, 1997)
11. Porcine (Brands, 2002)
12. Porcine (Miller, 1997)
13. Infant pig (Thibault, 1998)
14. In vivo pig (Miller, 2000)
15. In vivo human (Manduca, 2001)
16. Human & Porcine (Author)

Modeling Results: Shear Linear Behavior

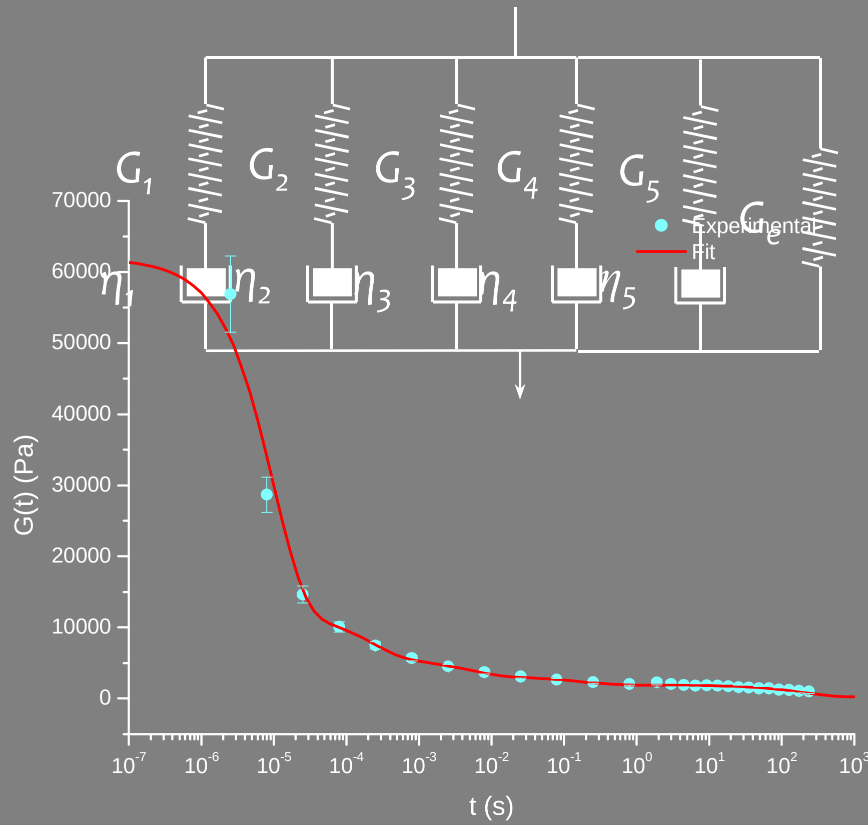

Time Domain

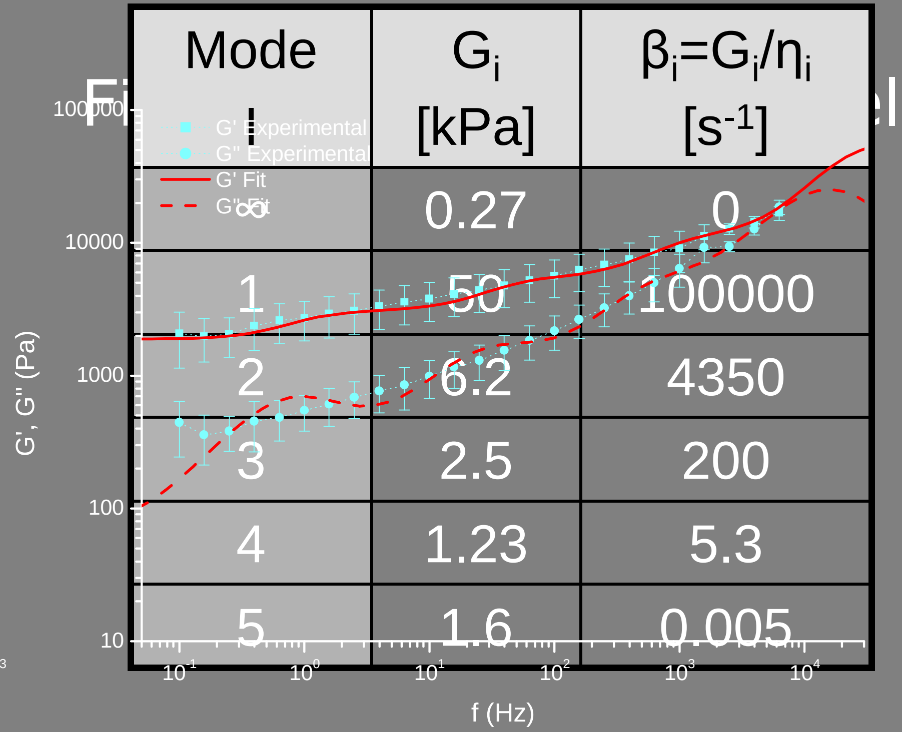

Mode i	G_i [kPa]	$\beta_i = G_i/\eta_i$ [s^{-1}]
∞	0.27	0
1	50	100000
2	6.2	4350
3	2.5	200
4	1.23	5.3
5	1.6	0.005

Frequency Domain

Analysis of the Shear Strain Softening of Brain Tissue

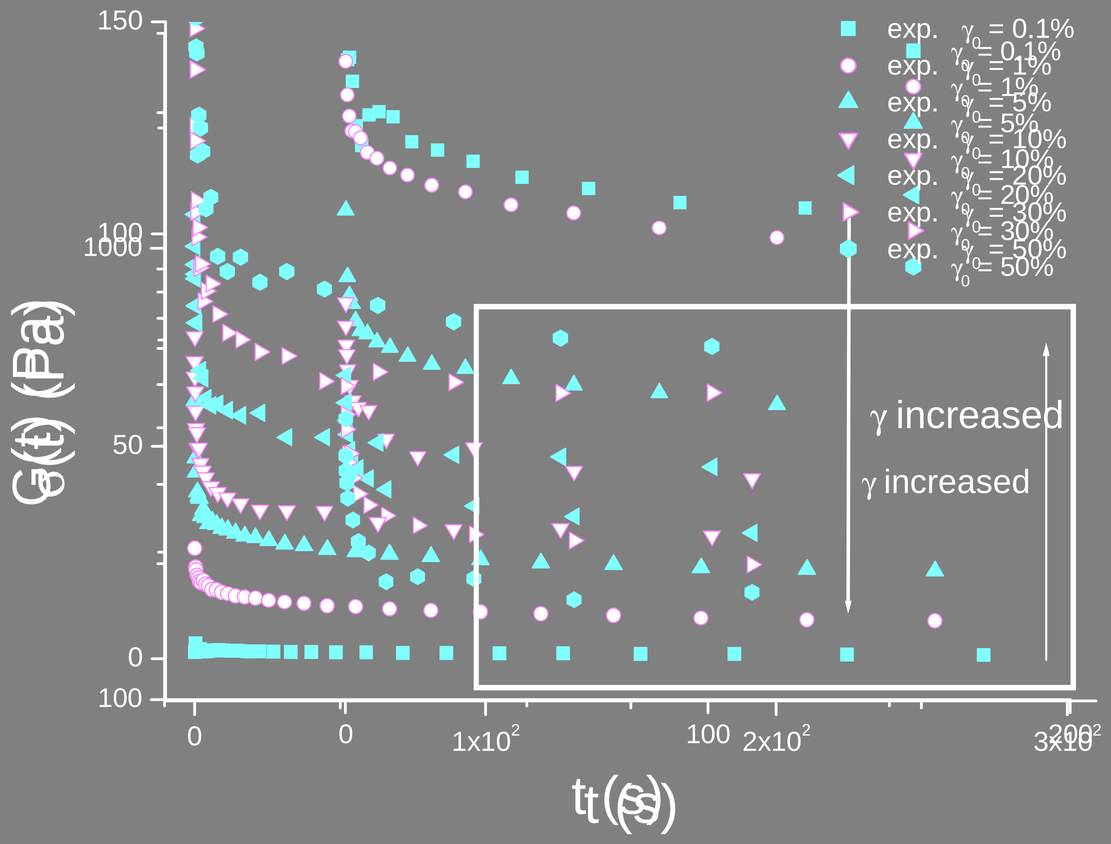

Hyperelastic Model

Hypothesis

- Reference State: Linear State
- Incompressibility: G(~1000 Pa) << K(~2.1 GPa)
- Isotropy: Low degree of anisotropy of the *Corona Radiata*
- Absence of Hysteresis Effects: (McElhaney, 1976 ; Mendis, 1995 ; Miller, 1997 and 2000 ; Brands, 2000 ; Prange, 2000)

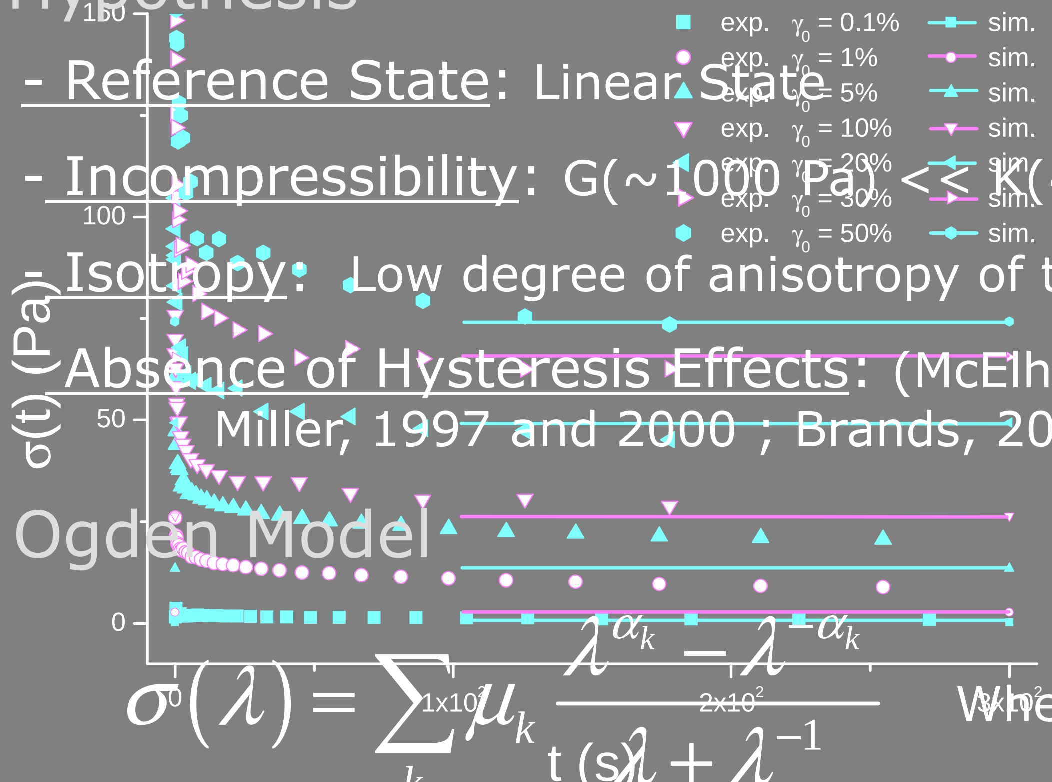

Ogden Model

$$\sigma(\lambda) = \sum_k \mu_k \frac{\lambda^{\alpha_k} - \lambda^{-\alpha_k}}{\lambda + \lambda^{-1}}$$

Where $\lambda = \frac{\gamma}{2} + \sqrt{1 + \frac{\gamma^2}{4}}$

Rang k	1	2	3
μ_k	60000	560	1.25
α_k	0.0451	-3.9	16.3

Towards a Visco-Hyperelastic Model

Hypothesis

- Time/Strain Factorization: Time-Dependant Behavior Is Independent of the Applied Strain

- At Long Times: $\sigma(\lambda, t \to \infty) = \sum_k \mu_k^e \frac{\lambda^{\alpha_k} - \lambda^{-\alpha_k}}{\lambda + \lambda^{-1}}$

- At Small Strain: Generalized Maxwell

$$\sigma(t)_{norm} = \frac{\sigma(\lambda,t)}{\sum_{k=1}^{3} \mu_k^e \frac{\lambda^{\alpha_k} - \lambda^{-\alpha_k}}{\lambda + \lambda^{-1}}} = \left(1 + \sum_{j=1}^{3} C_j e^{-t/\tau_j}\right)$$

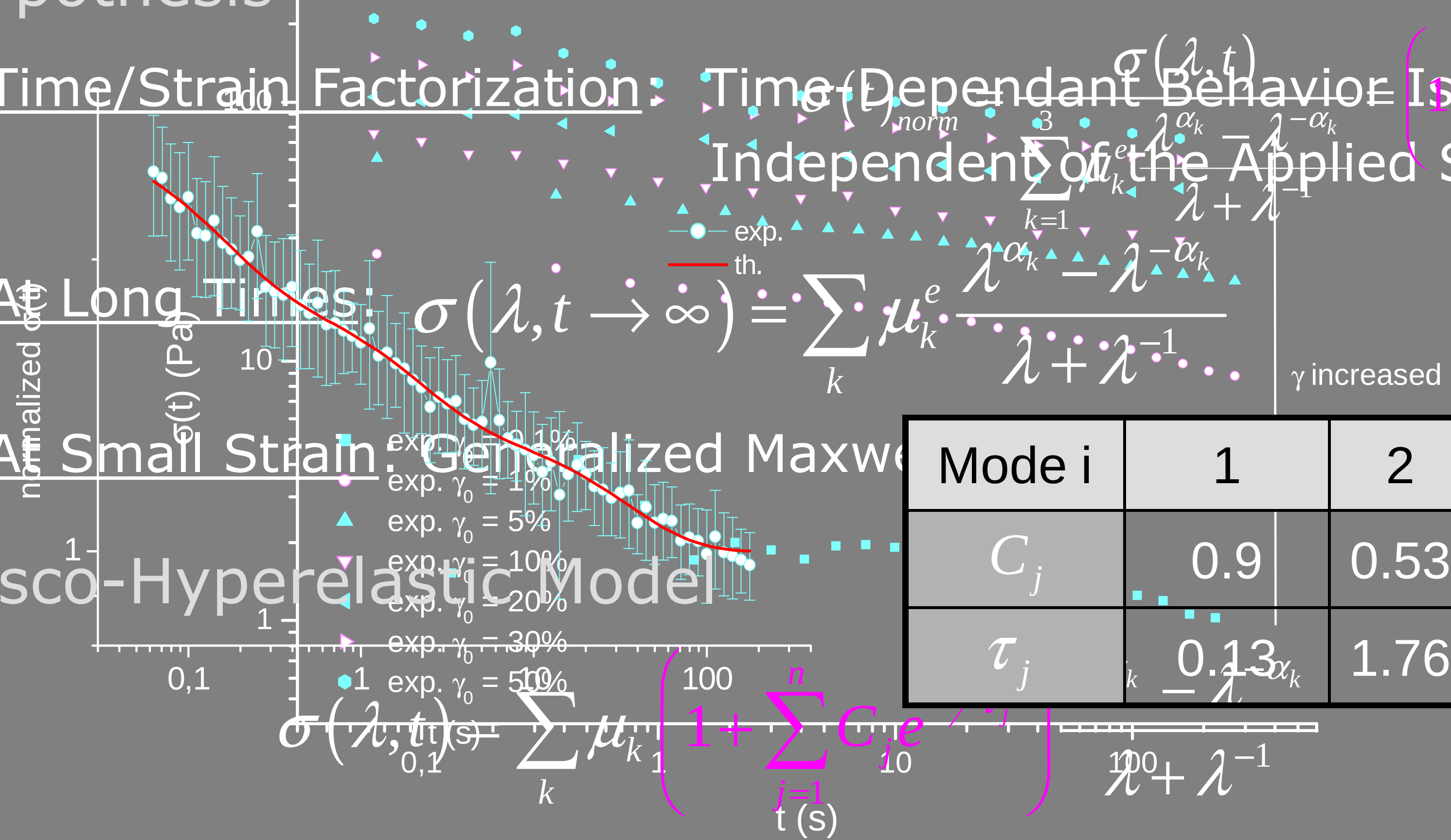

Mode i	1	2	3
C_j	0.9	0.53	0.4
τ_j	0.13	1.76	31

Visco-Hyperelastic Model

$$\sigma(\lambda,t) = \sum_k \mu_k \left(1 + \sum_{j=1}^{n} C_j e^{-t/\tau_j}\right) \frac{\lambda^{\alpha_k} - \lambda^{-\alpha_k}}{\lambda + \lambda^{-1}}$$

Towards a Visco-Hyperelastic Model

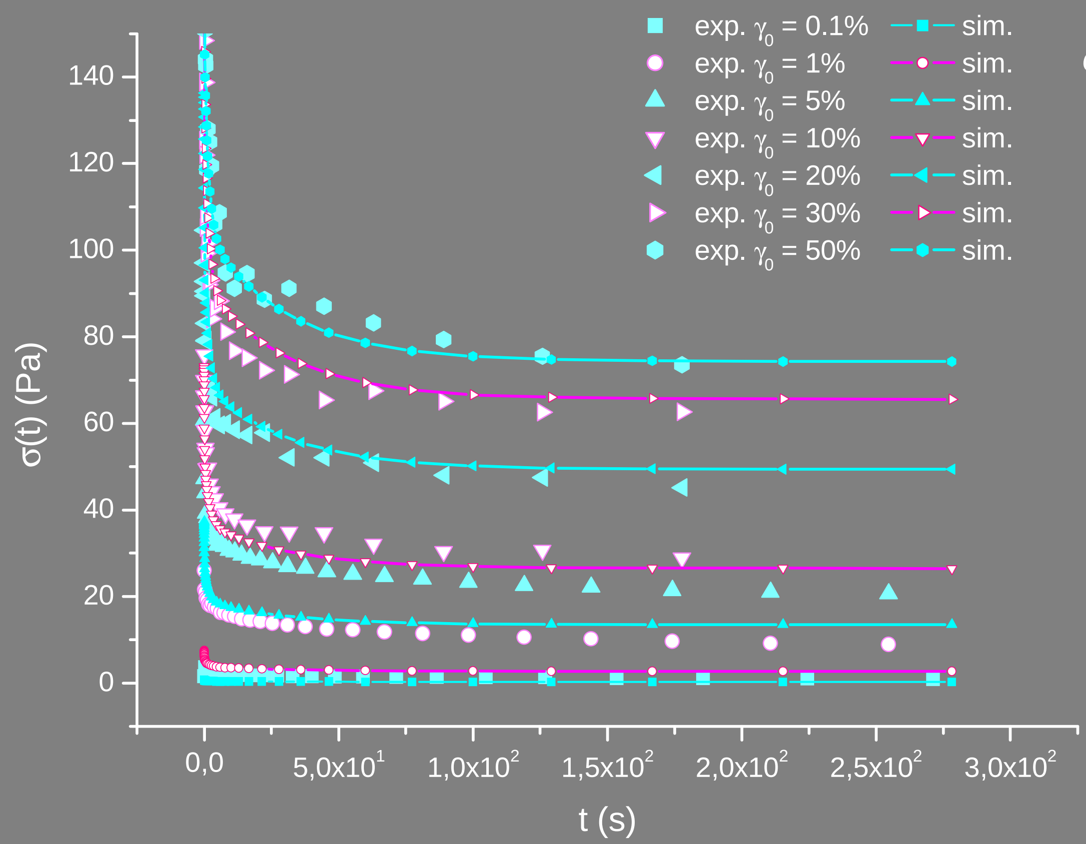

$$\sigma(\lambda,t)=\sum_k \mu_k\left(1+\sum_{j=1}^{n} C_j e^{-t/\tau_j}\right)\frac{\lambda^{\alpha_k}-\lambda^{-\alpha_k}}{\lambda+\lambda^{-1}}$$

Rang k	1	2	3
μ_k	60000	560	1.25
α_k	0.0451	-3.9	16.3

Mode i	1	2	3
C_j	0.9	0.53	0.4
τ_j	0.13	1.76	31

CARACTERISATION DU CERVEAU IN VIVO

In vitro tests : Validation on ex-vivo porcine brains

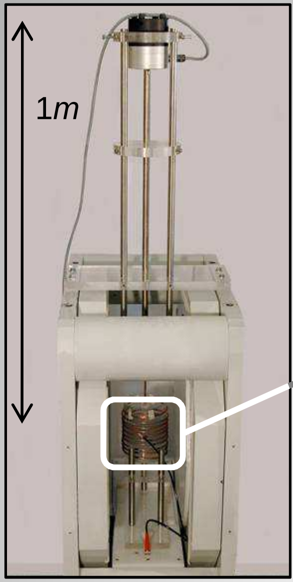

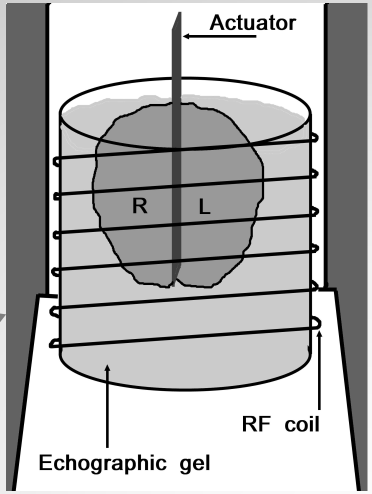

Vertical MRE Experimental device for ex vivo porcine brain

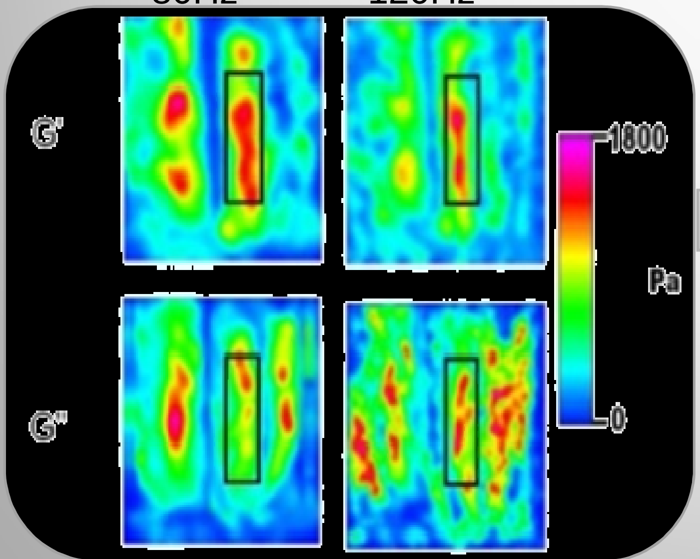

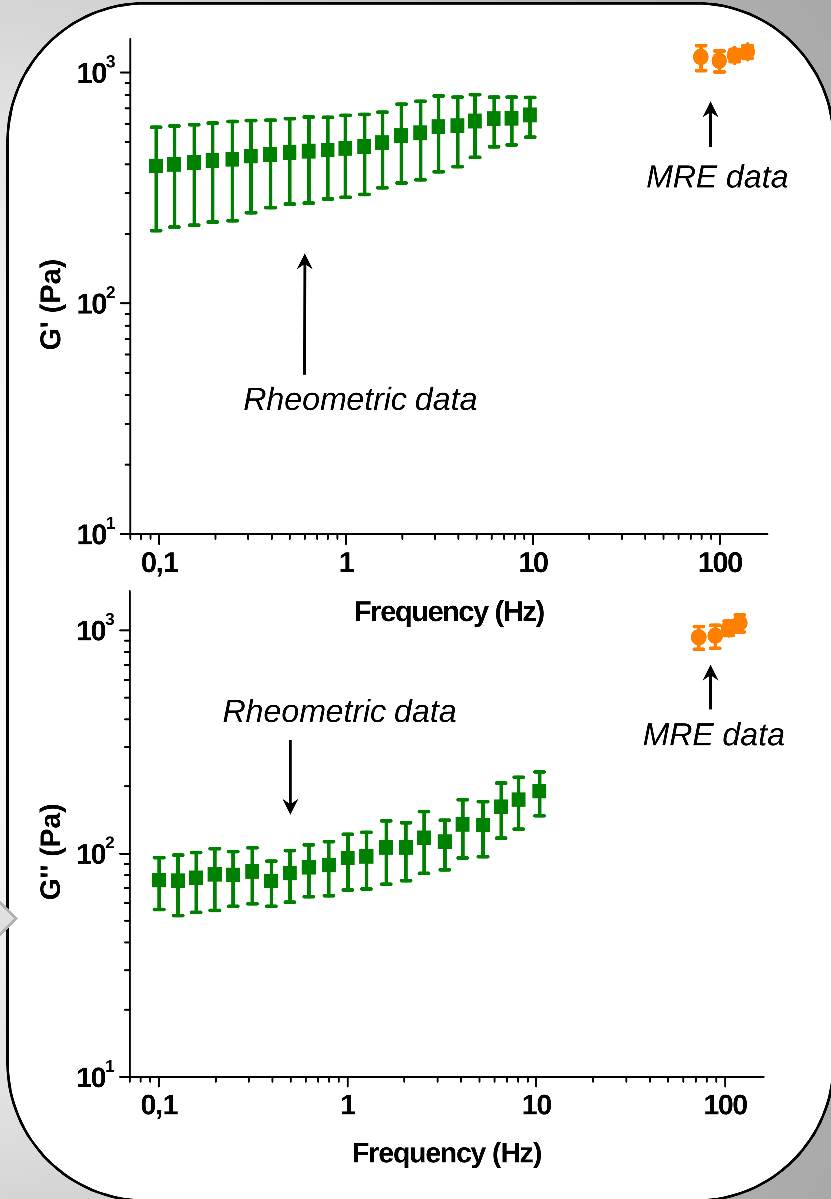

In vivo tests : preliminary results on 7 rats

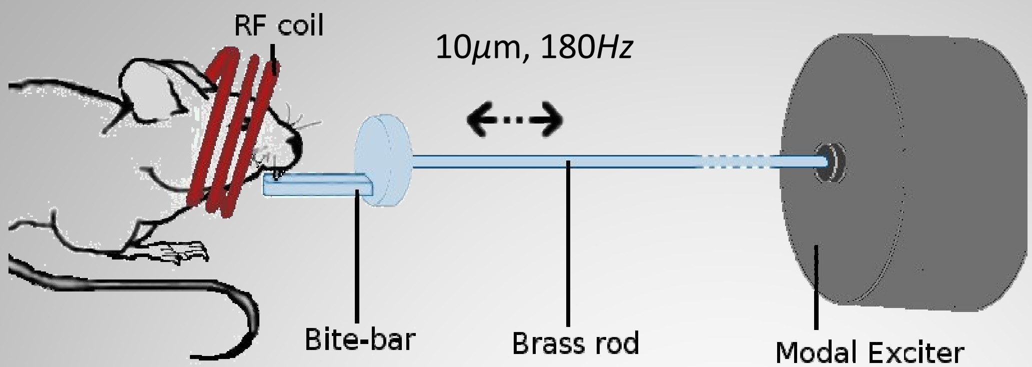

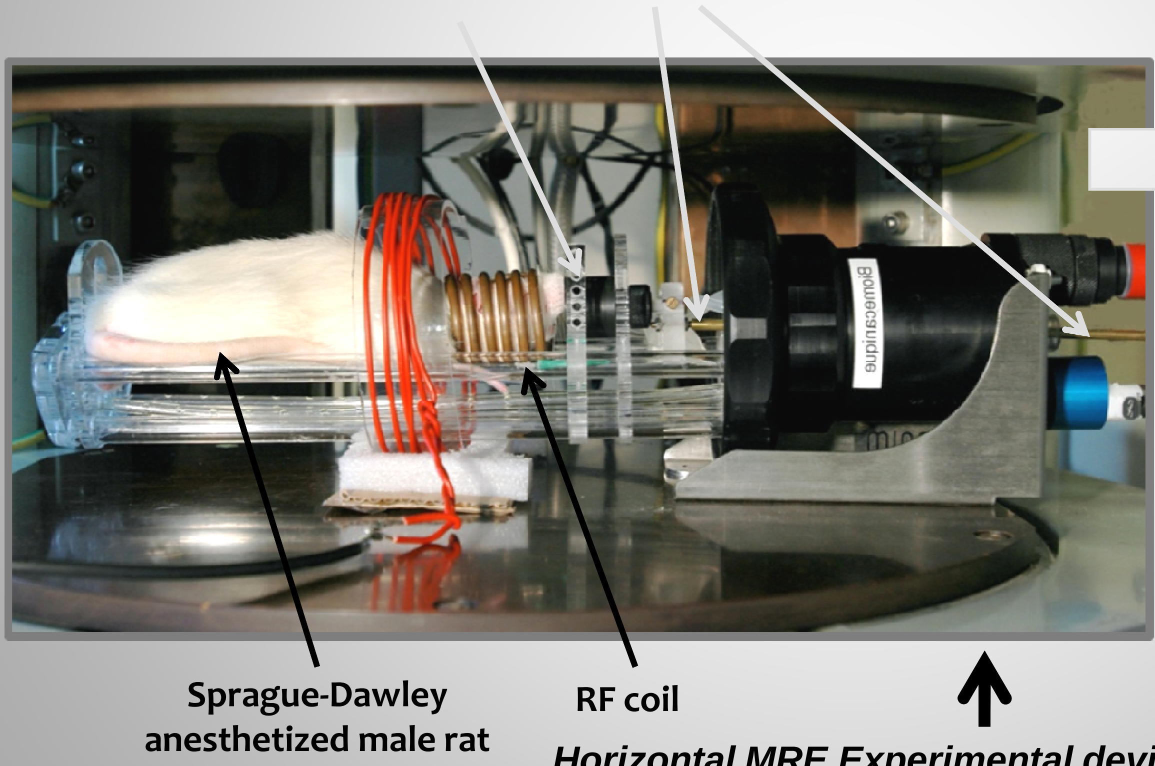

Horizontal MRE Experimental device for* in vivo *rat brain

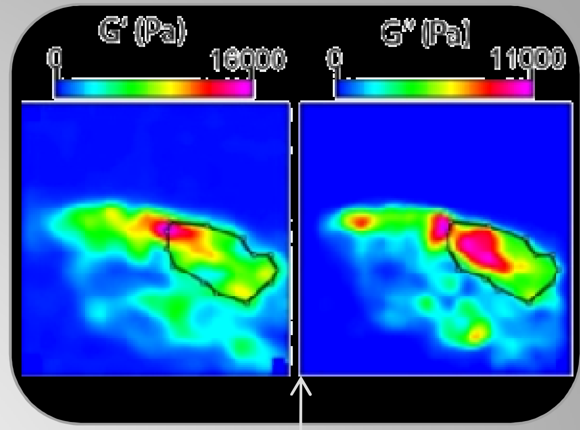

Rat brain distribution maps of G' and G" with a manually selected region of interest

Mean shearing moduli at 180*Hz* for the 7 tested rats :

$$G' = 7600 \pm 650 Pa$$

$$G'' = 7500 \pm 1600 Pa$$

Limite de tolérance au choc

HUMAN SEGMENTS

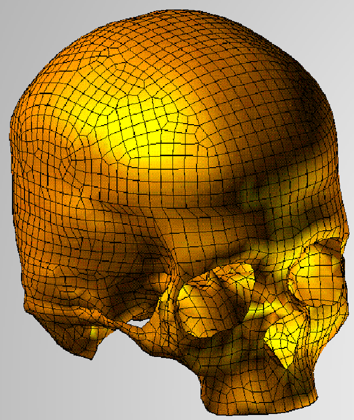

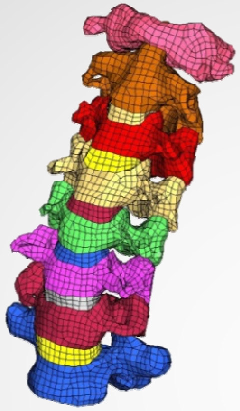

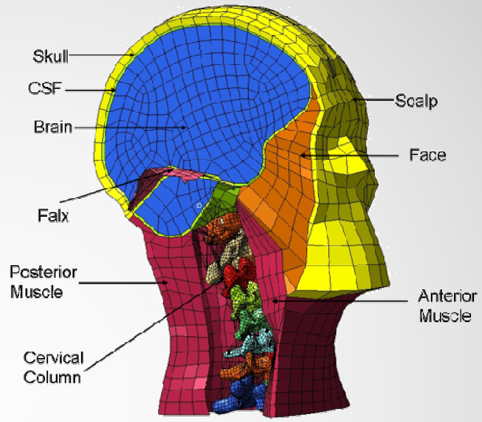

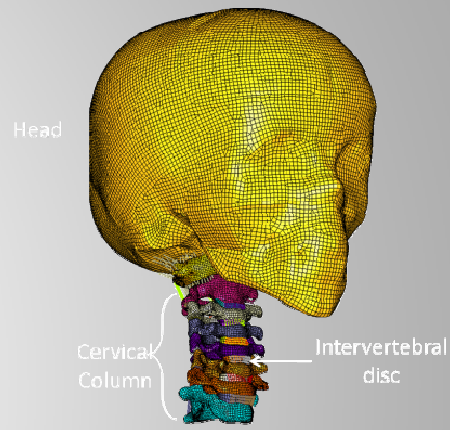

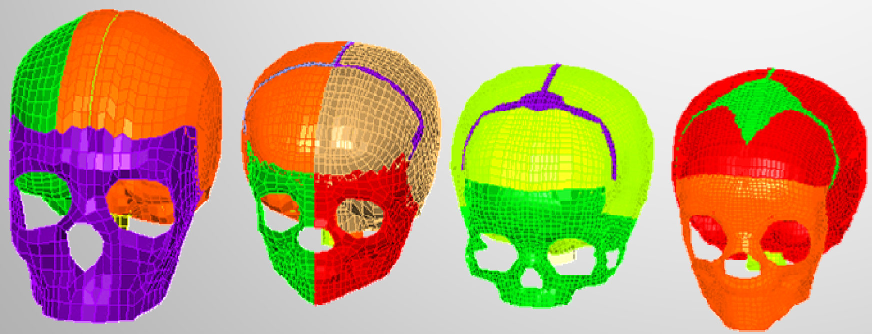

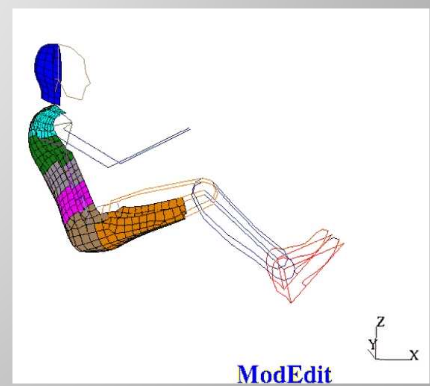

Biomécanique du Traumatisme Crânien

- Aspect historique
- Modélisation et validation du modèle de la tête
- Limites de tolérances spécifiques à un mécanisme

Existing Head Injury Criteria

- Head substitute: Headform mass of M = 4.5 to 4.8 kg
- Injury mechanism related to linear head acceleration
- Based on cadaver head tests(Wayne State University 1960)

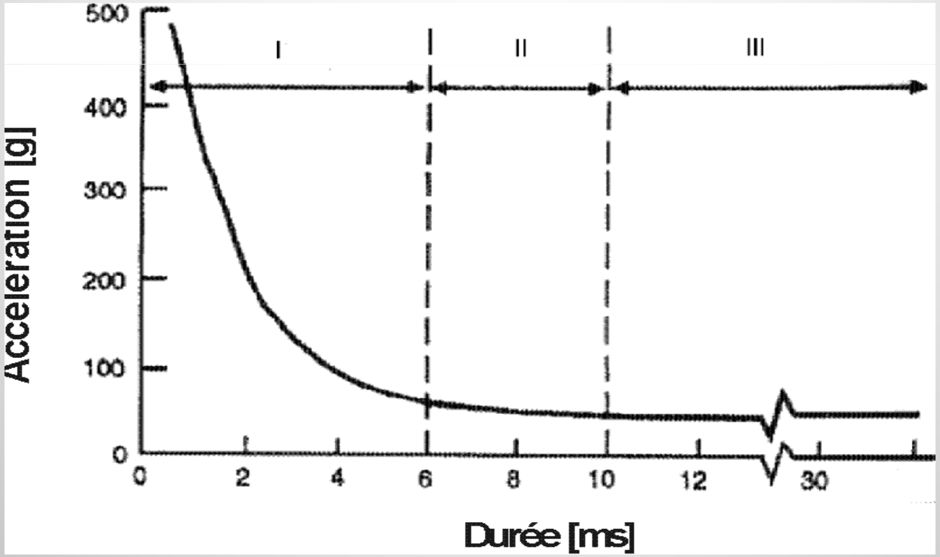

Wayne State Tolerance Curve

Head Injury Criteria (HIC, 1972)

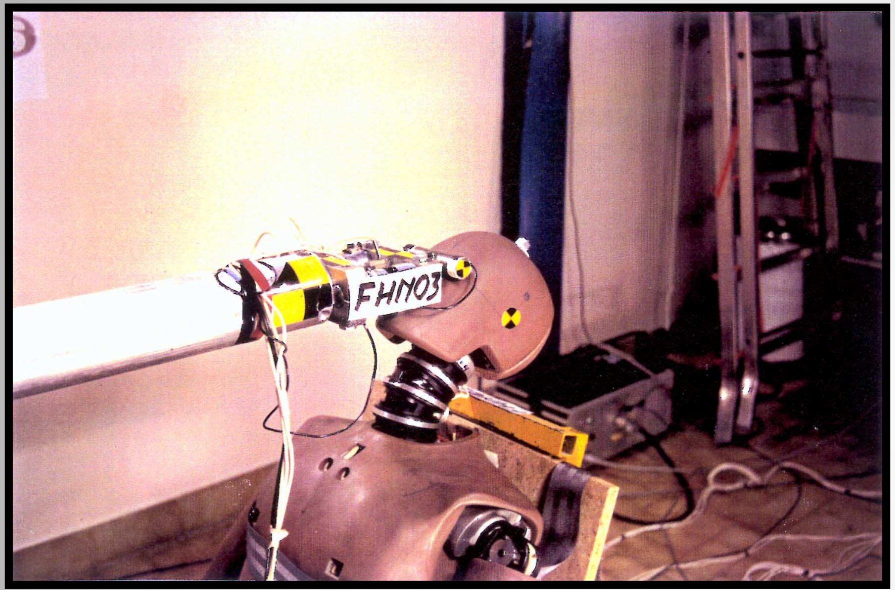

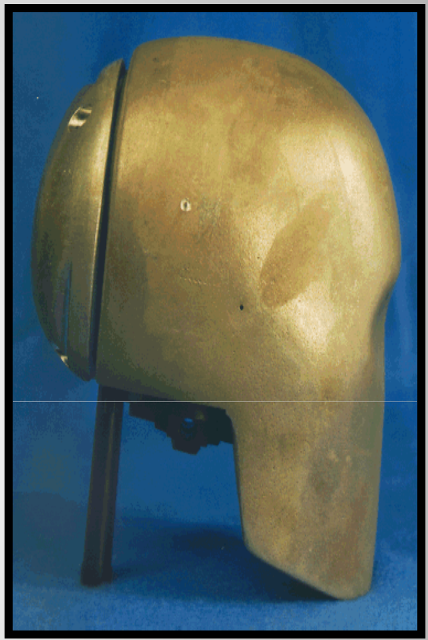

$$HIC = (t_2 - t_1)\left[\frac{1}{(t_2 - t_1)}\int_{t_1}^{t_2} a\,dt\right]^{2.5}$$

M = 4.58 kg

HIC = 1000

Limites du HIC

- Non prise en compte de l'accélération rotatoire

- Non direction dépendant

- Ne tiens pas compte des mécanismes de lésion

HEAD INJURY MECHANISMS AND RELATED PARAMETER

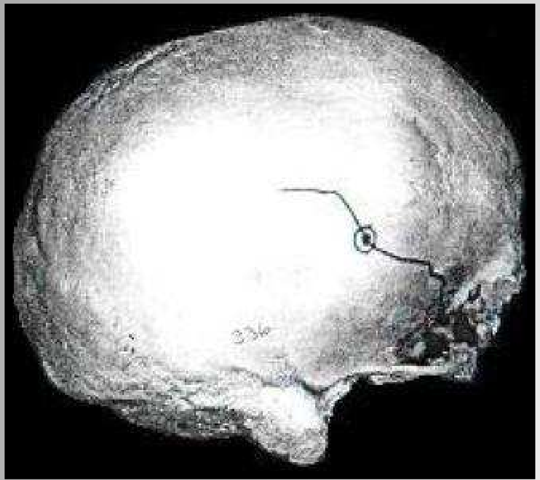

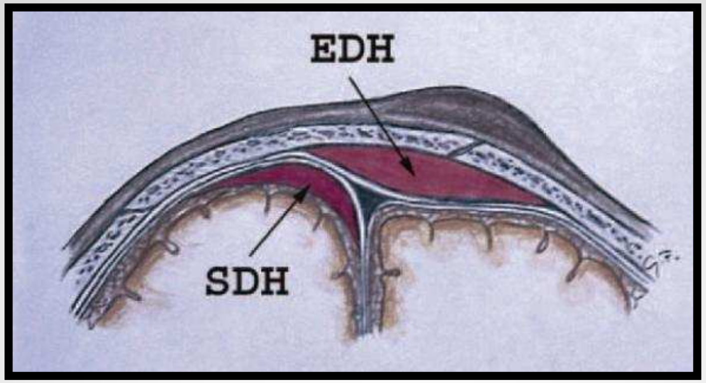

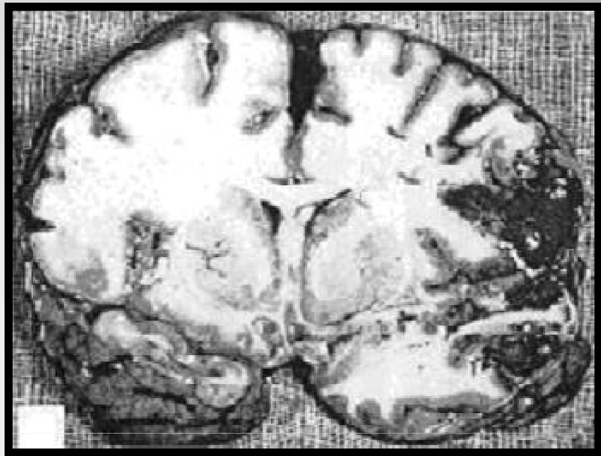

Skull fractures ⟷ Skull deformation

Subdural and subarachnoidal haematoma ⟷ Relative motion between the brain and the skull

Diffuse Axonal Injuries (DAI) ⟷ Intracerebral strains/stress

STRASBOURG UNIVERSITY FE HEAD MODEL

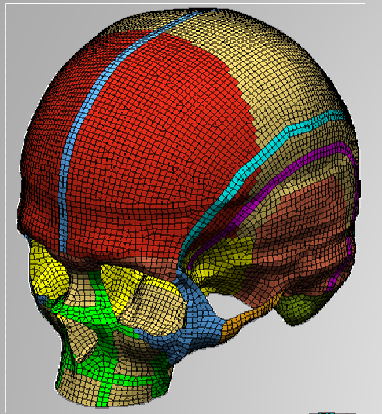

Outer table

Falx

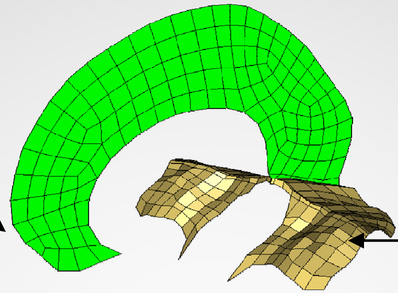

Tentorium

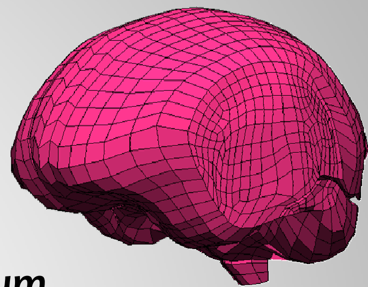

Brain

Diploë

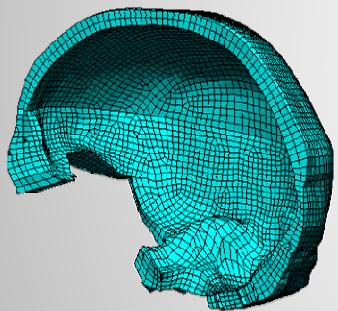

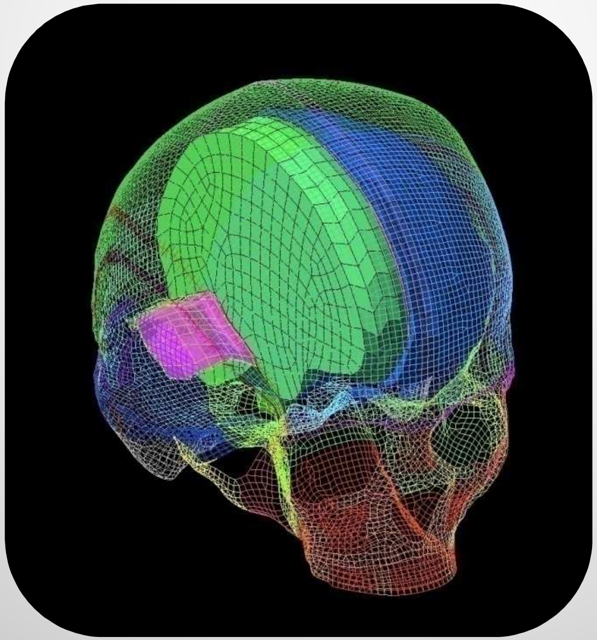

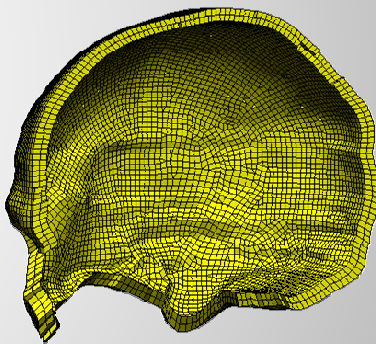

Scalp

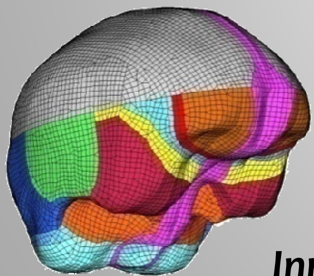

Inner table

48266 bricks

25977 shell

74243 elements

Nahum Experimental Impact(1977)

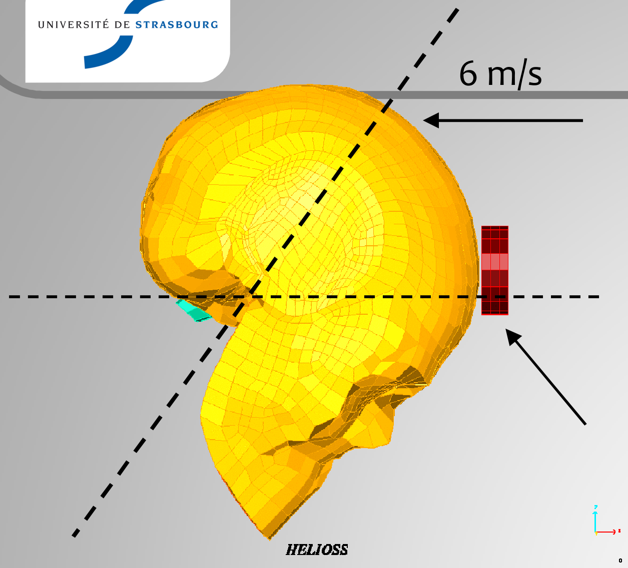

IMPACTOR

MASS 5.6Kg

E=13.6 Mpa

ν=0.16

Validation parameters

- Impact force
- Linear Head acceleration
- Five intracranial-pressure

Head acceleration

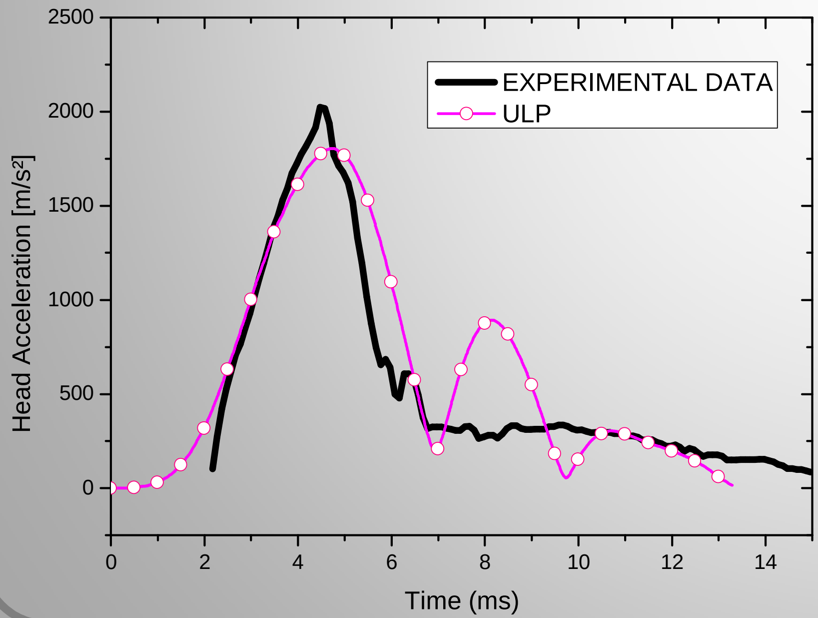

Impact Force

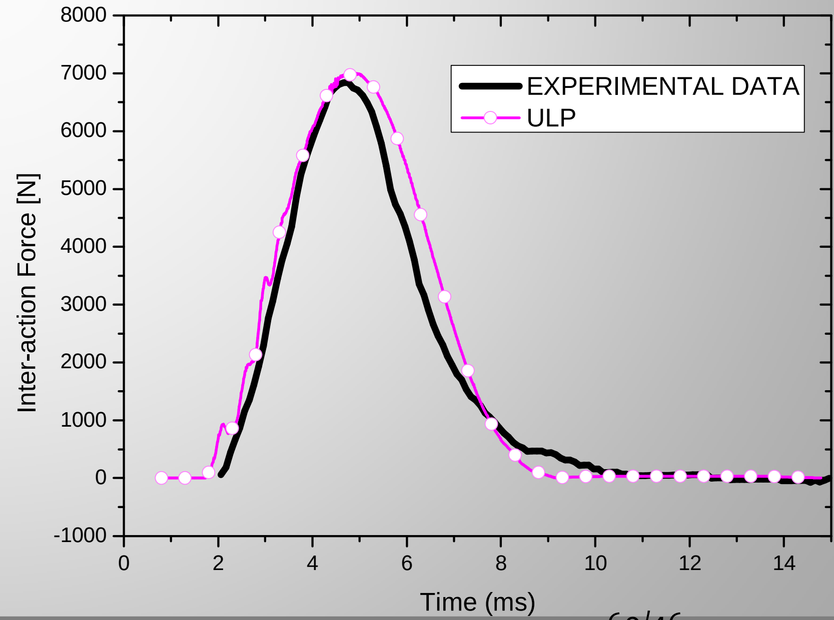

NAHUM (1977)

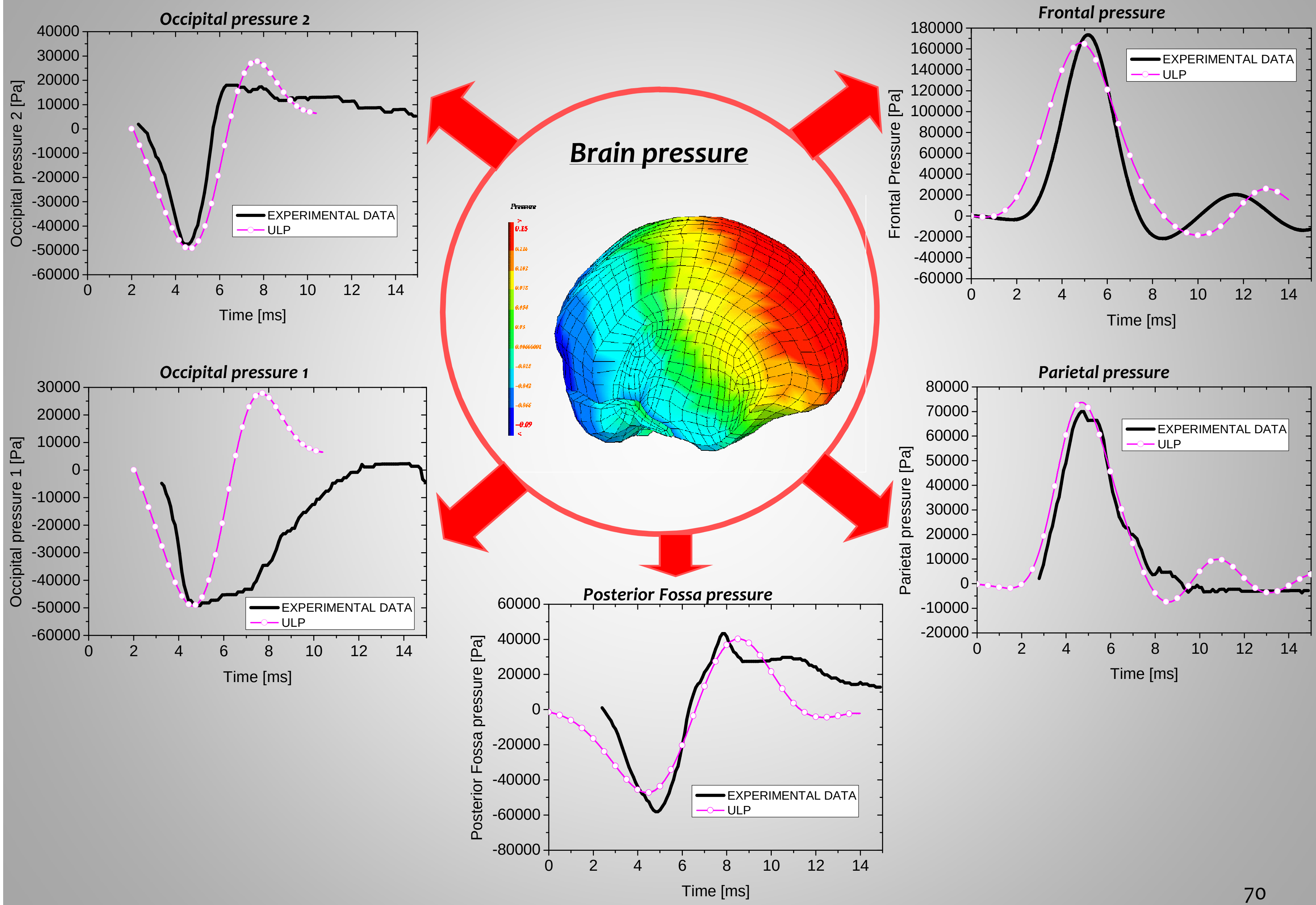
Occipital pressure 2
Occipital pressure 2 [Pa]
Time [ms]
EXPERIMENTAL DATA
ULP
Occipital pressure 1
Occipital pressure 1 [Pa]
Time [ms]
EXPERIMENTAL DATA
ULP
Brain pressure
Pressure
Frontal pressure
Frontal Pressure [Pa]
Time [ms]
EXPERIMENTAL DATA
ULP
Parietal pressure
Parietal pressure [Pa]
Time [ms]
EXPERIMENTAL DATA
ULP
Posterior Fossa pressure
Posterior Fossa pressure [Pa]
Time [ms]
EXPERIMENTAL DATA
ULP

MS428-2 case

TROSSEILLE (1992)

INPUT

Linear accelerations

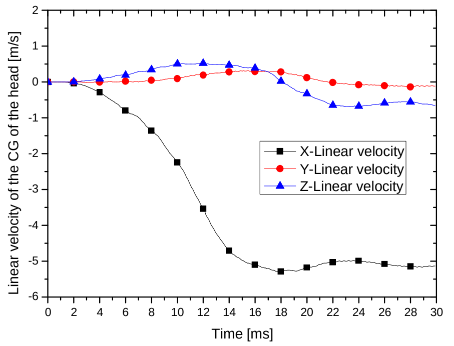

Rotational accelerations

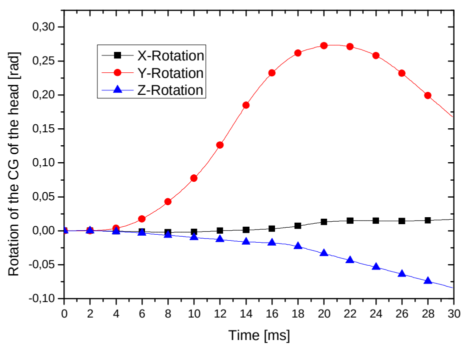

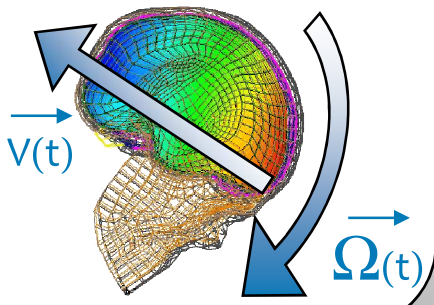

OUTPUT (3 accelerations, 5 pressures)

ACCELERATION

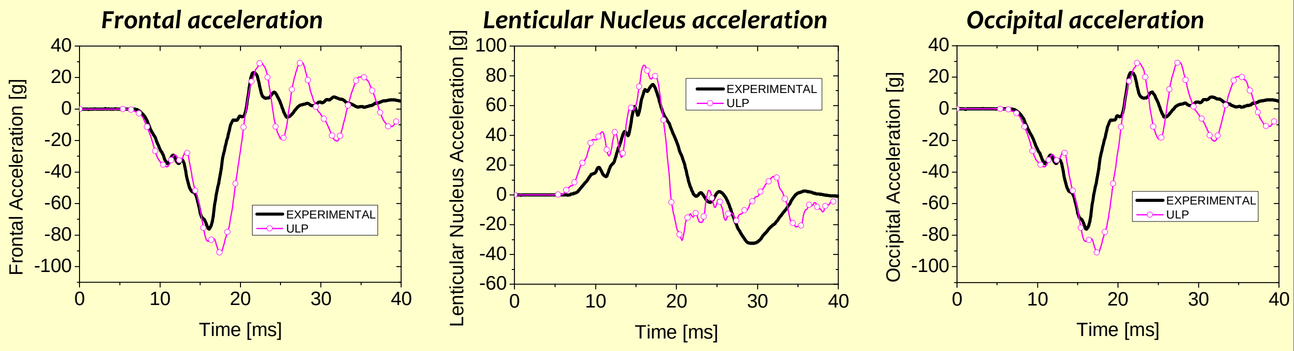

PRESSURE

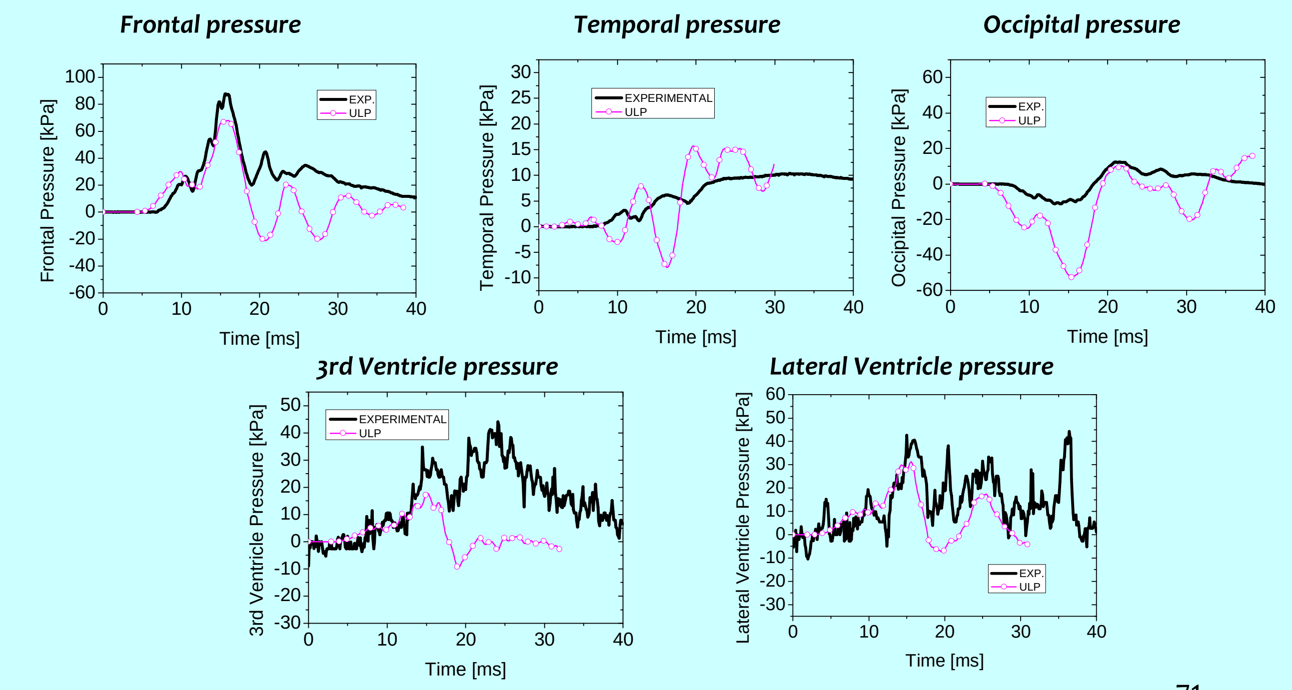

Occipital impact (C755-T2)

HARDY (2001)

INPUT

Linear accelerations

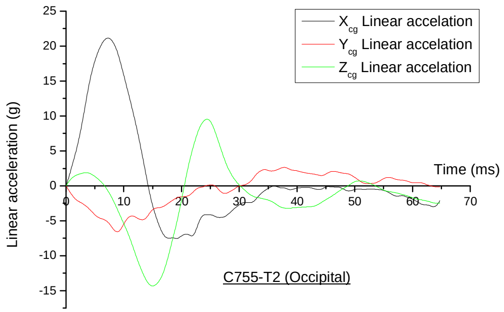

Rotational accelerations

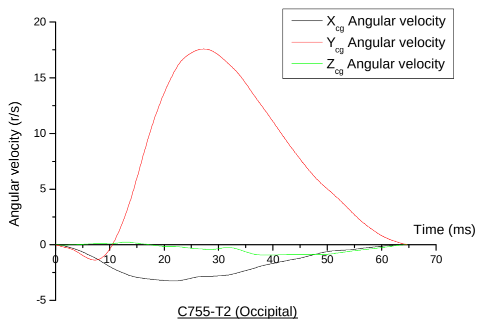

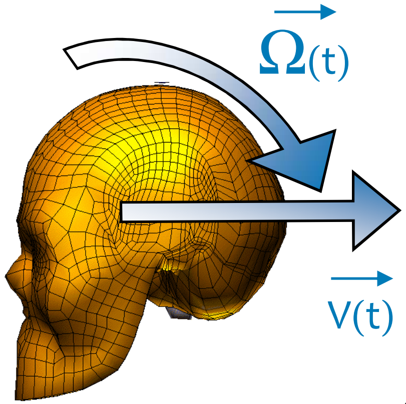

OUTPUT

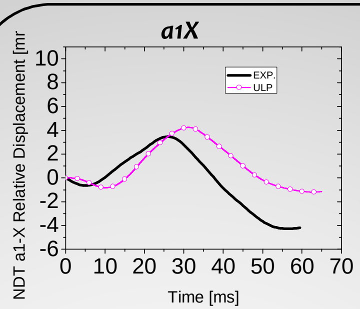

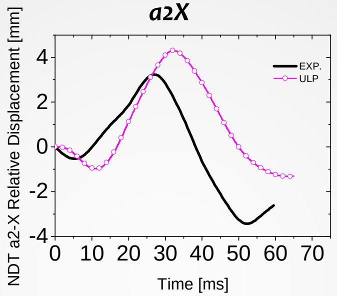

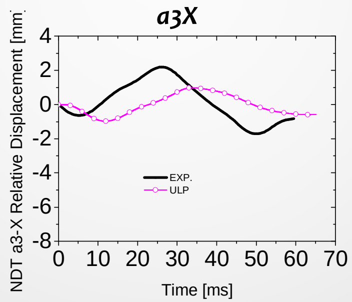

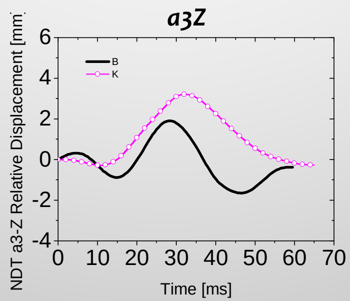

NDT's displacement

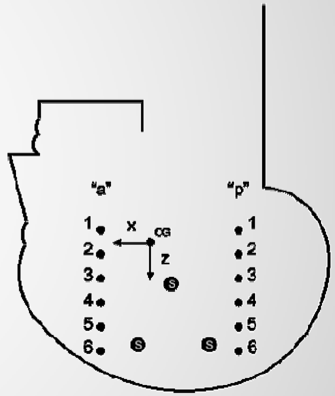

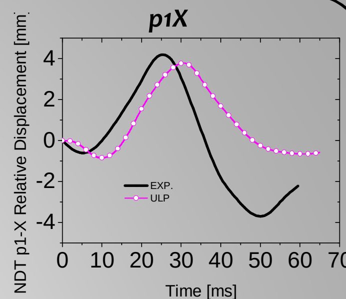

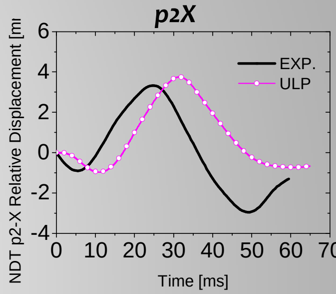

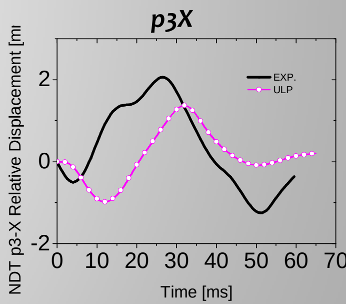

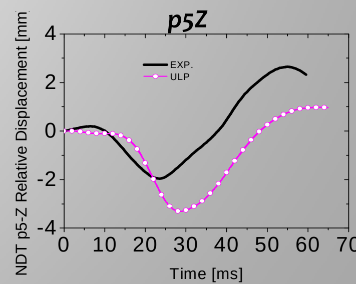

Simulation de Trauma Crâniens

MODEL BASED INJURY CRITERIA

Experimental or analytical replication

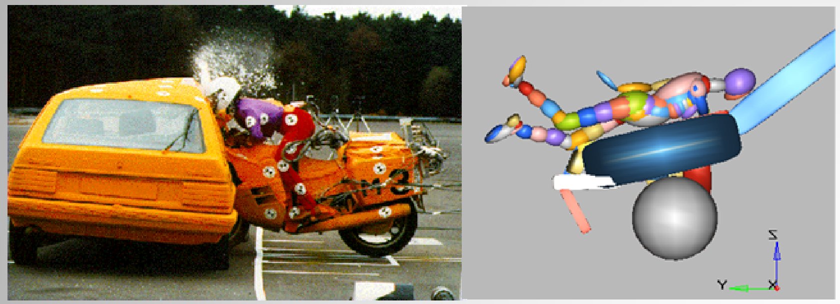

Real accidents

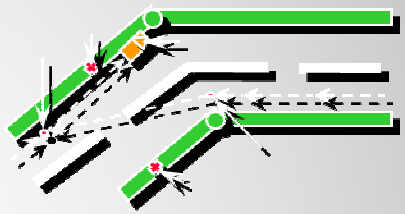

Detailed medical report

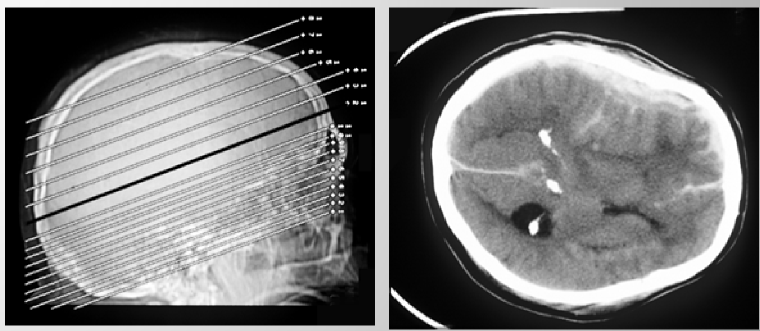

Numerical reconstruction

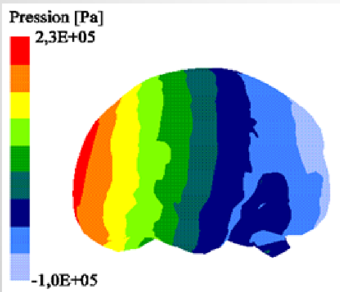

Injury mechanisms and tolerance limits

Modelling of the Protection Systems

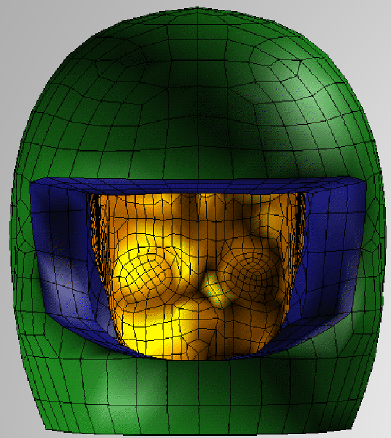

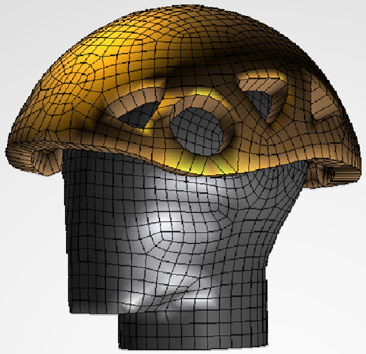

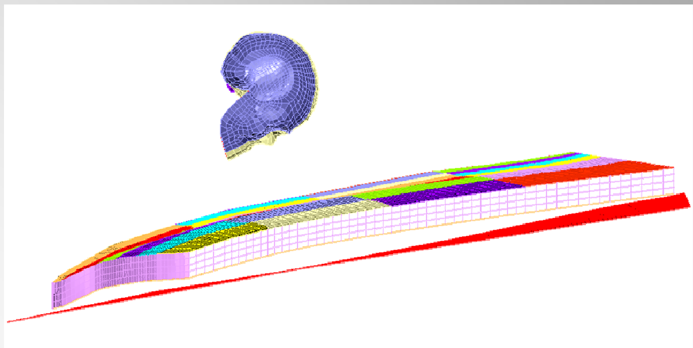

Motorcyclist

Cyclist

Pedes

Balistic

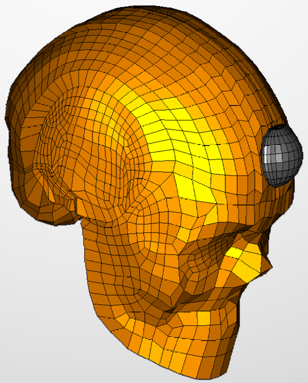

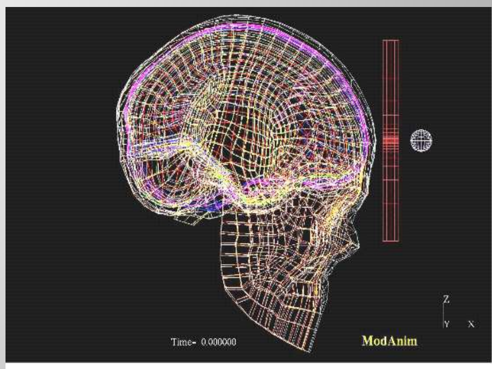

EXTRACTION OF CRITERIA

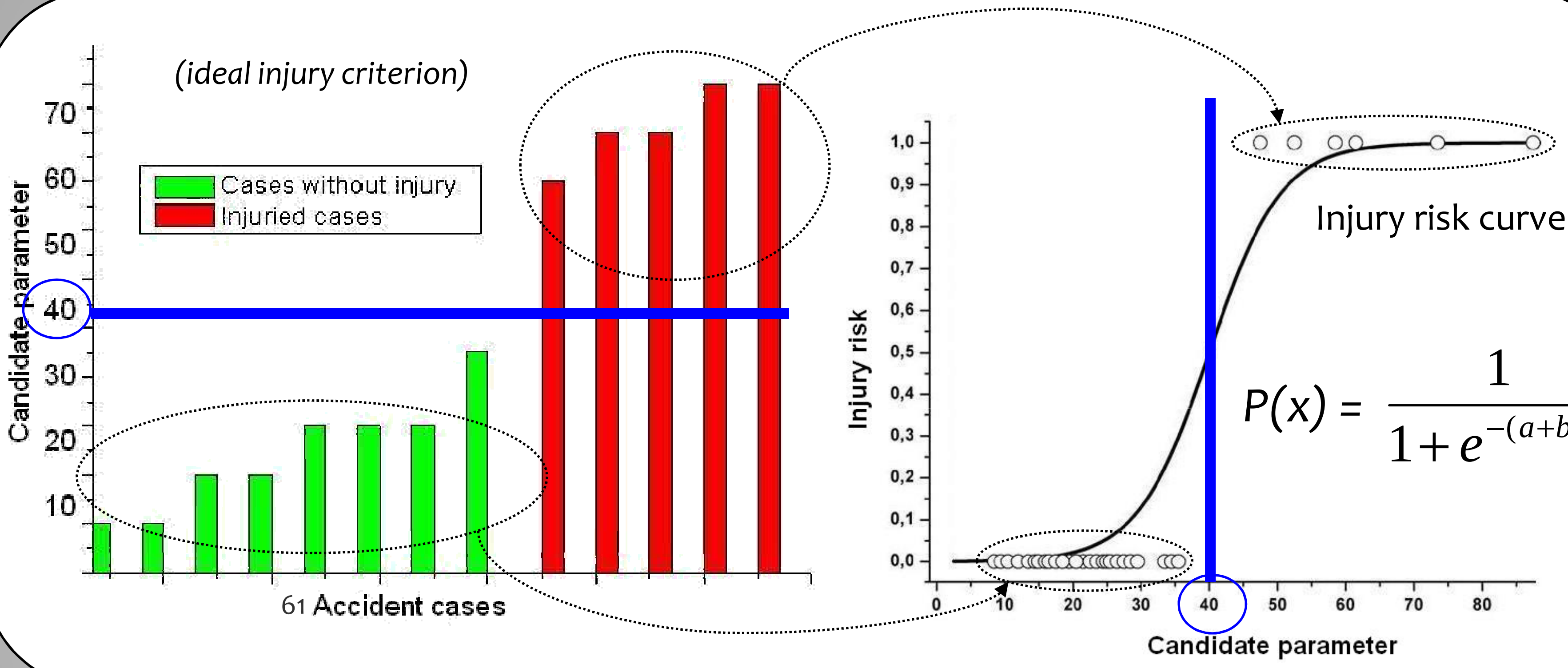

$$P(x) = \frac{1}{1+e^{-(a+bx)}}$$

Binary logistic regression (SPSS v14.0)

Nagelkerke R-sq statistic

HEAD INJURY MECHANISMS AND RELATED PARAMETER

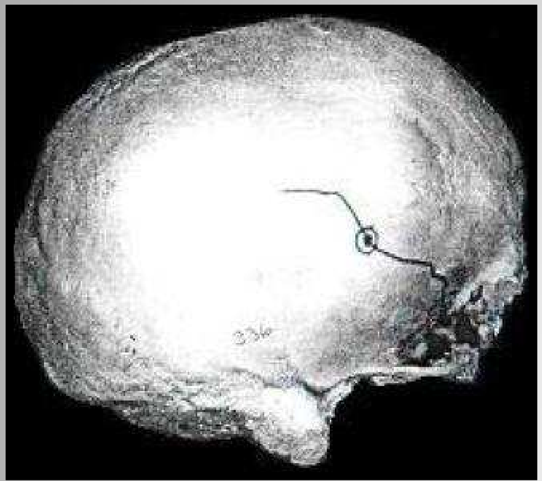

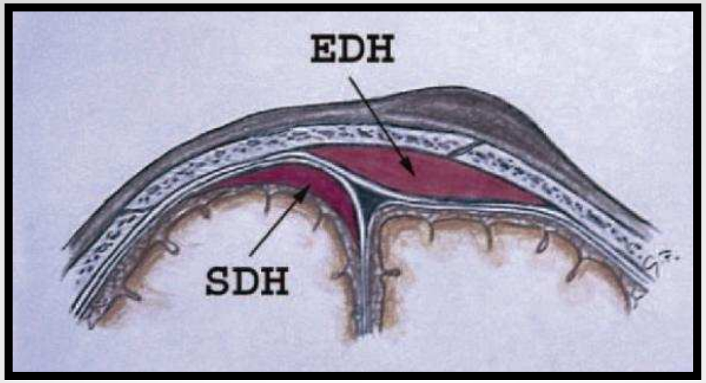

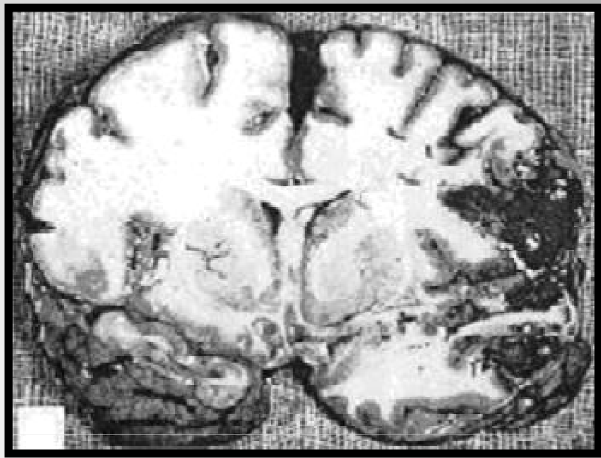

Skull fractures ⇕ Skull deformation

Subdural and subarachnoidal haematoma ⇕ Relative motion between the brain and the skull

Diffuse Axonal Injuries (DAI) ⇕ Intracerebral strains/stress

UdS TOLERANCE LIMIT TO SKULL FRACTURE

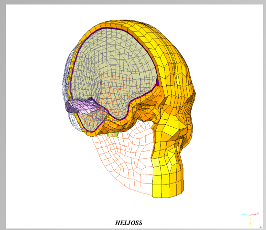

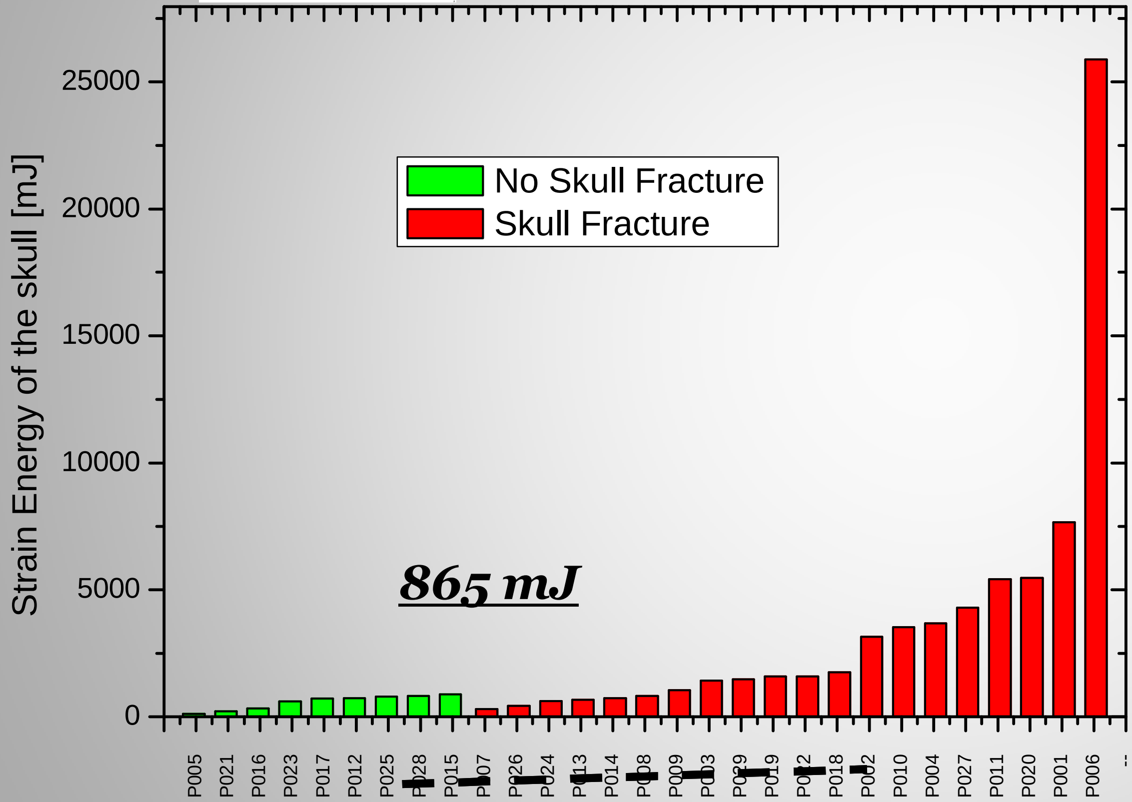

Bone injuries

Skull fracture

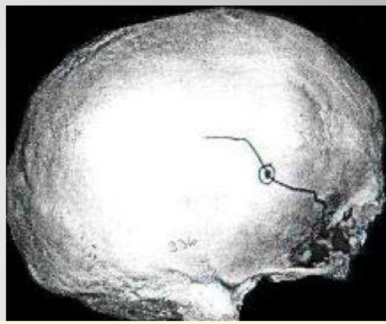

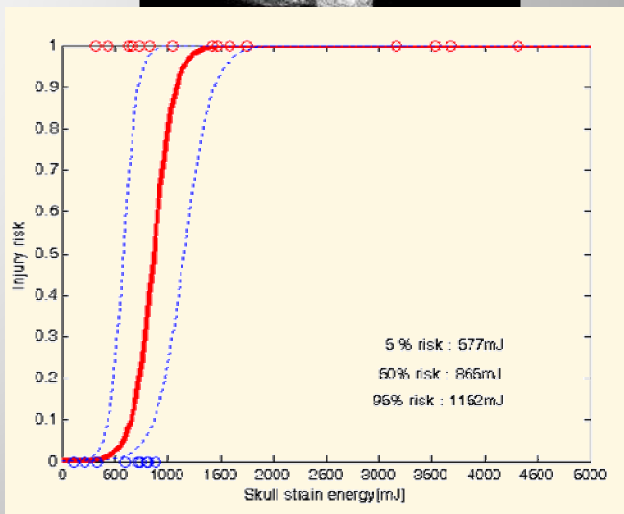

UdS TOLERANCE LIMIT TO SDH

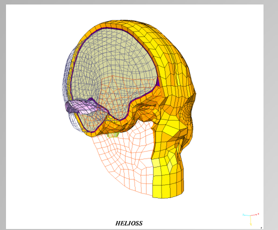

Vascular injuries

Subdural hematoma

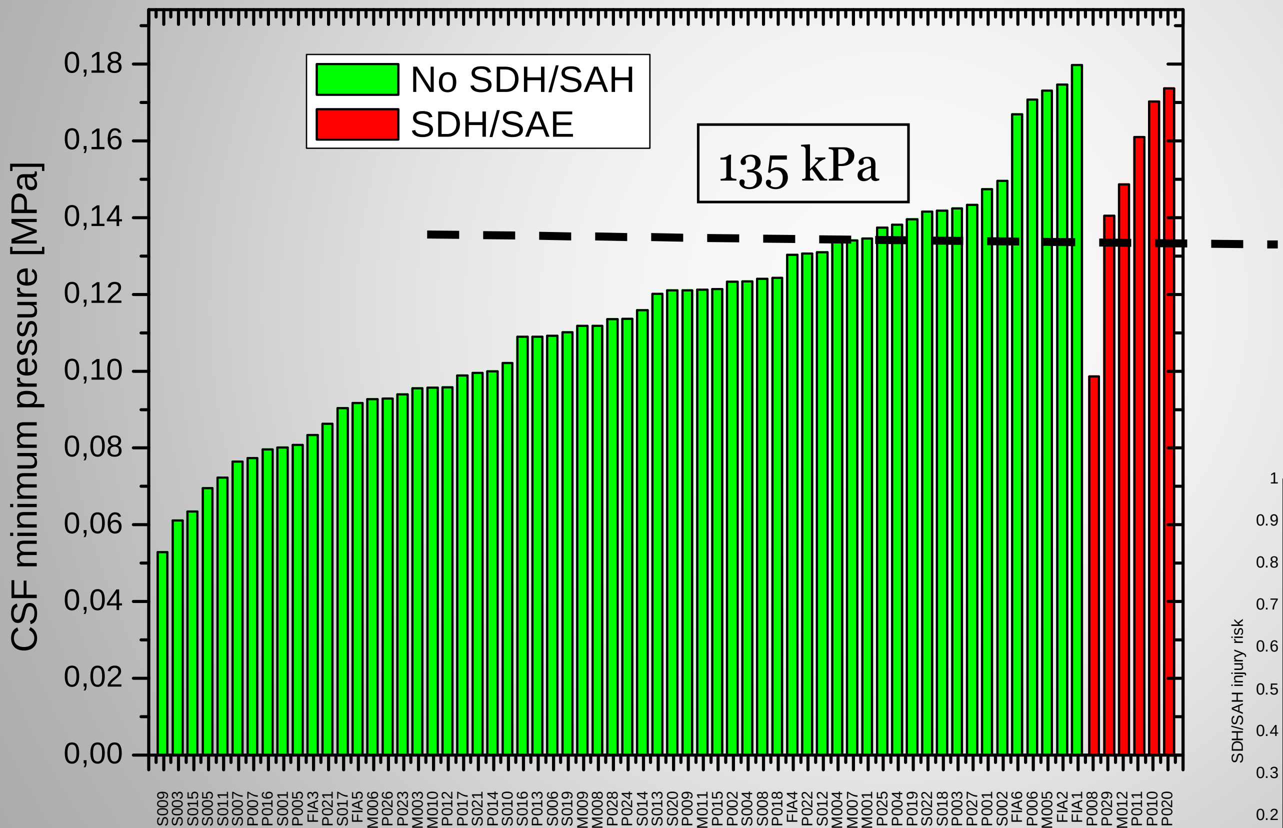

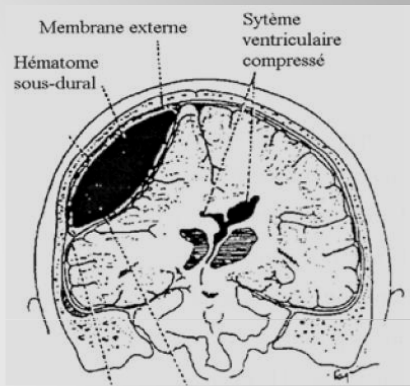

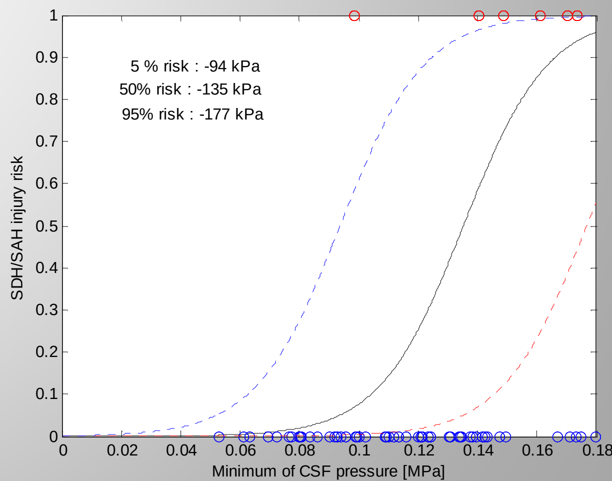

UdS TOLERANCE LIMIT TO DAI

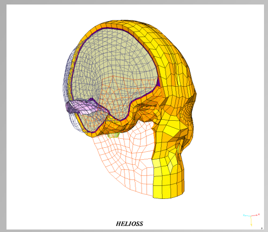

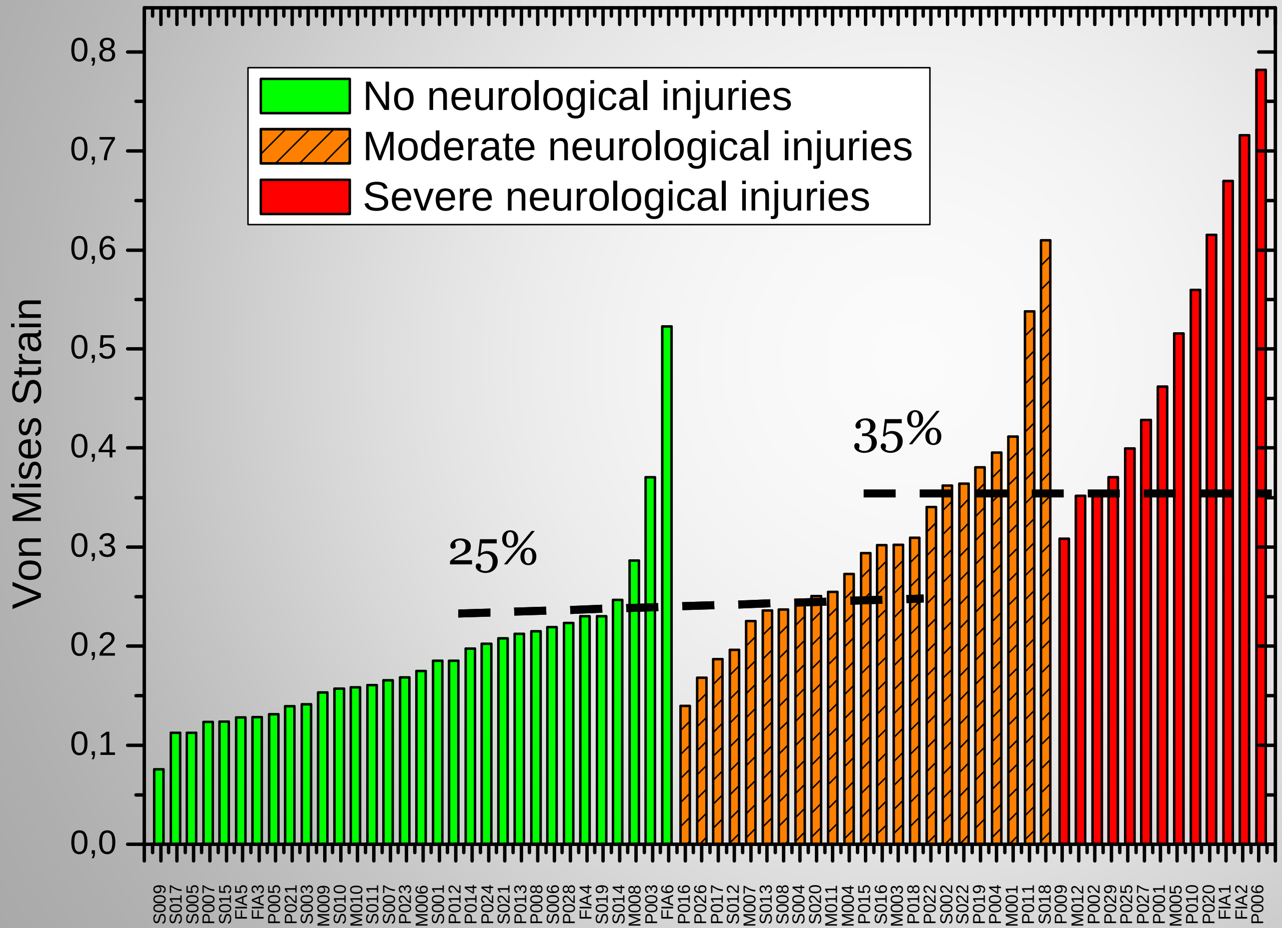

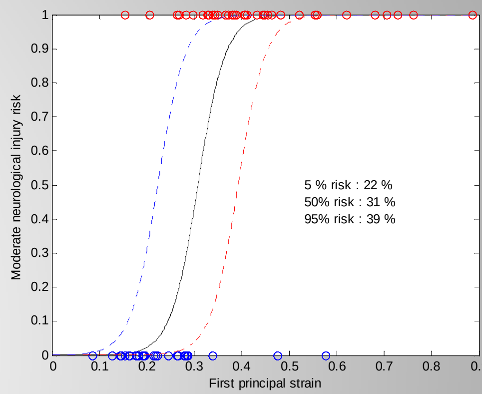

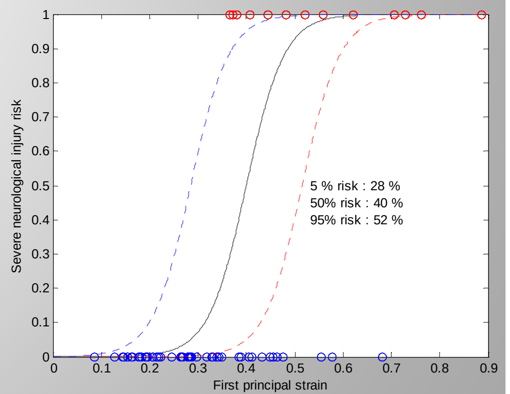

UdS HEAD INJURY CRITERIA

- Sub-arachnoidal haematoma (50% risk)
  - CSF Minimum pressure : 135 kPa
- Moderate neurological injuries (50% risk)
  - Intra-cerebral Von Mises stress > 26 kPa
  - Intra-cerebral Von Mises strain > 25 %
- Severe neurological injuries (50% risk)
  - Intra-cerebral Von Mises stress > 33 kPa
  - Intra-cerebral Von Mises strain > 35 %
- Skull fractures (50% risk)
  - Global strain energy of the skull > 0.865 J

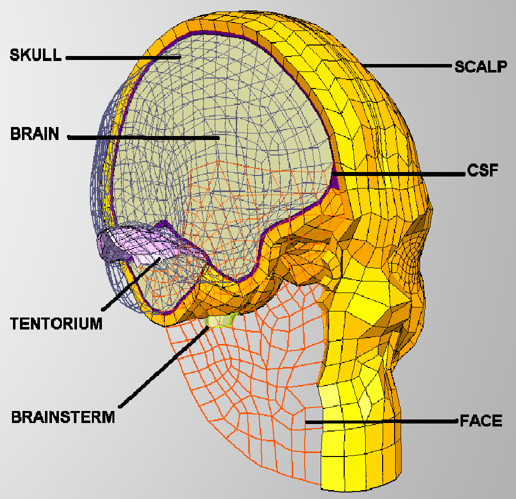

Développements futurs

- Investigations in vivo (humain et aniimal)
- Caractérisation aux grandes déformations
- Anisotropie / hétérogénéité
- Effets des vaisseaux sanguins et pressurisation
- Limites de tolérance sur modèle animal

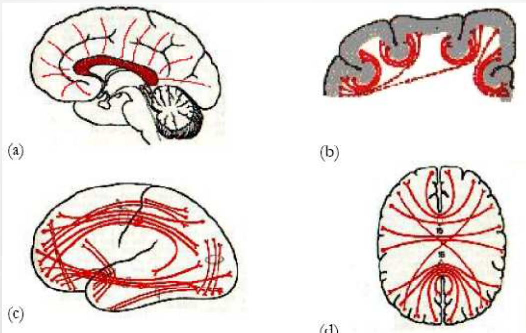

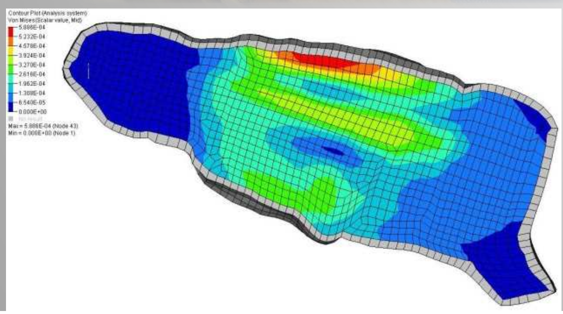

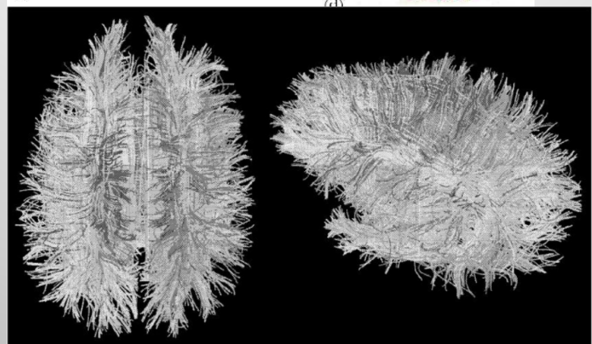

Remerciements

Chatelin S, Constantinesco A.,

Deck C., Kang H. Nicolle S.,

Oudry J, Soleur L., Vappou J

IRCAD, ENSPS

Références

Nicolle S., Lounis M., Willinger R : Shear properties of brain tissue over a frequency range relevant for automotive impact situations : New experimental data. Stapp Car Crash J. 2004, Vol 48, 239-258

Nicolle, S., Lounis, M., Willinger, R. and Palierne J-F. (2005). Shear Linear Behavior of Brain Tissue over a Large Frequency Range. Biorheology 42(3), 209-223.

Vappou J., Willinger R., Breton E., Choquet P., Goetz C., Constantinesco A., "Dynamic viscoelastic shear properties of soft matter by Magnetic Resonance Elastography using a low-field dedicated system", J. Rheol, 2006, Vol 50, Issue 4, pp531, 541.

Vappou J., Breton E, Choquet P, Goetz C., Willinger R., Constantinesco A. : Magnetic resonance elastography compared with rotational rheometry for in vitro brain tissue viscoelasticity measurment. Accepté dans MAGMA en decembre 2007.

Vappou J., Breton E., Choquet P., Willinger R., Constantinesco A. : Assessment of in-vivo and post-mortem mechanical behaviour of brain tissue using magnetic resonance elastography. J Biomech. 2008, Vol 41, pp2954-2959.

Deck C, Willinger R : Improved Head Injury Criteria Based on Head FE Modeling. Int J of Crashworthiness, 2008, Vol 13, N°6, pp 667-679.

Oudry J, Bastard C., Miette V., Willinger R., Sandrin L : Copolymer-in-oil phantom materials for elastography. Ultrasound in Med & Biol. 2009, Vol 35, N7, 1185-1197.

J. Oudry, J. Vappou, P. Choquet, R. Willinger, L. Sandrin, and A. Constantinesco, Ultrasound-based Transient Elastography compared to Magnetic Resonance Elastography in soft tissue-mimicking gels, Phys Med Biol, 2009, N°54, 6979-6990.

Oudry J, J. Chen, K.J. Glaser, V. Miette, L. Sandrin, R.L. Ehman, Cross-Validation of Magnetic Resonance Elastography and Ultrasound-Based Transient Elastography: A Preliminary Phantom Study, J Magn Res, accepted, 2009

GDR STIC-Santé : Biomécanique des Tissus Mous, Lyon 26 Novembre 2009

Caractérisation exérimentale et modélisation de tissus biologiques

remy.willinger@imfs.u-strasbg.fr

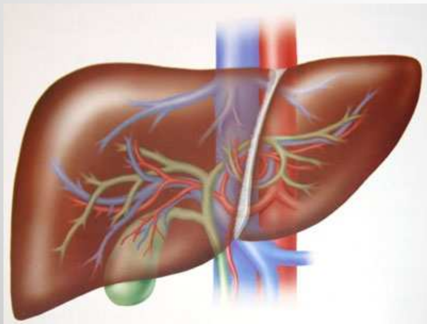

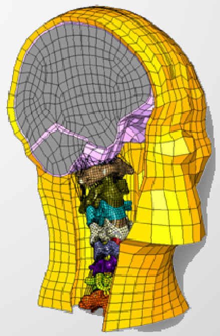

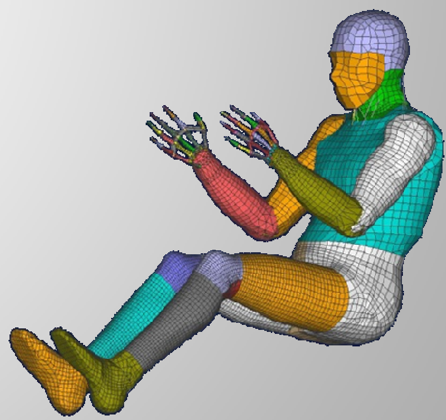

Rémy Willinger[a]

University of Strasbourg, IMFS-CNRS, Strasbourg, France